Crystal Growth, Characterization, and Point Contact Spectroscopy on Cu_xTiSe_2

by

Mike Potalivo

A THESIS SUBMITTED IN PARTIAL FULFILMENT OF
THE REQUIREMENTS FOR THE DEGREE OF

MASTER OF SCIENCE

in

The Faculty of Mathematics and Sciences

Department of Physics

BROCK UNIVERSITY

June 16, 2010

Abstract

Various sets of single crystals and poly crystals of Cu_xTiSe_2 were grown. X-ray diffraction and energy dispersive spectroscopy results verified that the crystals were the correct composition and crystal structure. Resistivity measurements and magnetic susceptibility measurements determined the superconducting transition temperatures for the crystals. The crystals in each growth had various superconducting transition temperatures. Also, the measurements indicated that the crystals were inhomogeneous. Point contact spectroscopy experiments were employed on various single crystals. Inspection of the data indicated that the material has a single energy gap. A program was built utilizing the Levenberg-Marquardt method and theory on point contact spectroscopy to determine the superconducting energy gap. Plots of the superconducting energy gap at various temperatures were in disagreement with what was expected for a conventional superconductor.

Acknowledgements

First and foremost, I owe great thanks to Dr. Razavi as well as his past and present members of his research group. Dr. Razavi has sacraficed countless hours of his own time to assist me, teach me, as well as give me support, especially when I needed it. His insights and his practices have encouraged me to become a knowledgable, independent worker that has given me confidence to take on seemingly impossible tasks. I am very fortunate to have worked along side with Dr. Razavi because it has became all too clear that his work ethics and practices have rubbed off on me. This has helped me to become a more confident and ethical person. Traits such as these are precious and I am honoured to have developed these in the time here working with Dr. Razavi at Brock University.

In edition to this, I must extend my thanks to the department of physics for all of their assistance they have given me throughout my university career. Not only have they educated me, but they have been like friends at times more than educators. This has always made me comfortable at Brock and is probably why I decided to do a Masters in Physics in the first place. Aside from this, I must thank Dr. Samokhin, Dr. Bose, and Dr. Mitrovic for taking there time to help answer some of my theoretical questions/complications. No research is ever done independently, and their input has given me guidance and a more clear understanding of difficult technical theories.

During my research at Brock University, the machine shop, electronics shop, and glassblowers have put in their fair share of work for me. From giving me spare parts when something was broken, to taking months to work with me to build elaborate equipment, I must say thank you. No research would have been accomplished without a support team like this. I enjoyed my many talks with all of you guys, and Ryan I am sorry that I broke that brand new piece of equipment you built for me as I was bringing it to the laboratory to use it.

My parents, my soon to be parents, as well as my soon to be wife, Annie Lightheart, thank you all for your love and support you have given me. Your encouragement throughout my years of doing research has been a huge inspiration to me and I love you all. Thank you!

To everyone that has helped me directly or indirectly to accomplish this, thank you!

Contents

List of Tables

List of Figures

Chapter 1

Introduction

1.1 Cause of Interest

Charge density waves (CDW) as well as superconducting (SC) states are widely observed in transition metal dichalcogenide(TMD) materials of the 2H type[1, 2]. The two states are known to compete with each other in these materials[2]. Cu intercalated into $TiSe_2$ is the first material where a SC state is observed in the 1T type TMD[1, 2]. This system enables the first detailed study in which the SC state is observed after a suppression of the CDW through intercalation[3]. Therefore, it is of interest to investigate if the SC and the CDW states compete in this 1T system, just like in it's counterpart, the 2H system.

1.2 Properties of Cu_xTiSe_2

1.2.1 $TiSe_2$

TMDs come in two crystal structures. Regardless of which crystal structure, the chalcogenide atoms form two parallel sheets where the chalcogenide atoms in each sheet are in a hexagonal arrangement. The transition metal atoms exists inbetween these two sheets. For one of the crystal structures the transition metal atoms coordinate octahedrally. This is denoted as the 1T type crystal structure and $TiSe_2$ is of this type[1, 2, 3, 4, 5, 6, 7]. The crystal structure of $TiSe_2$ can be seen in figure 1.1 by neglecting the Cu atoms. For the 2H type, the transition metal atoms are in trigonal coordination with respect to each other. By looking at figure 1.1, the 2H structure can be visualized as a deviation from this one. The difference is the transition metals do not form a rectangular prism. The transition metal atoms in the ab, ac, and bc planes are not coordinating to form rectangles as before but are forming parallelograms. These faces of parallelograms construct the 3-dimensional image of the transition metal atoms coordination for the 2H type.

Woo et al. measured the Hall effect on $TiSe_2$ and found that the current carriers are electrons[8]. It is debated if $TiSe_2$ is a semimetal[8, 9, 10, 11] or semiconductor[2, 12, 13] at room temperature and some made reference stating that it could be either[3, 6]. Reason for this debate comes from various conclusions that have been

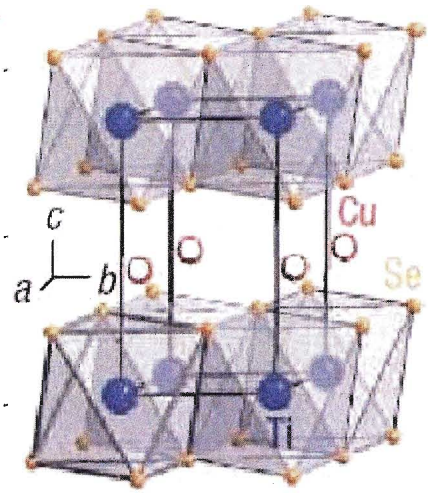

Figure 1.1: Crystal structure of Cu_xTiSe_2[3].

previously formed. Angle-resolved photoemission by Kidd et al. found that the material is a semiconductor because they detected a small indirect band gap in the band structure[12]. In addition, band structure calculations from Myron and Freeman indicates that $TiSe_2$ is expected to be a semiconductor[13]. However, angle-resolved photoemission by Bachrach and Skibowski did not agree. They argue that the material is semimetal as long as the stoichiometry is correct[9]. It has been noted that during the growth of $TiSe_2$, if the growth temperature is too high, this will reduce the stoichiometry by creating a lack of Ti[8].

At lower temperatures, $TiSe_2$ undergoes a phase transition into a CDW state. Salvo, et al. noted in their neutron-diffraction measurements that the phase transition occurs around 200K[10]. Woo et al. in x-ray diffraction experiments noted that the phase transition seemed to be of second order[8]. They also noted with x-ray diffraction experiments that the CDW is a (2a x 2a x 2c) wavevector with no incommensurate phase[8]. Kidd et al. also argued in their angle-resolved photoemission measurement that the CDW is caused by electron hole coupling together with a similar effect to the Jahn-Teller effect[12]. Holt et al. used their x-ray results to argue that the transition is caused by a Jahn-Teller effect[14]. Miyahara et al. performed tunneling spectroscopy on $TiSe_2$ which was used to determine the energy gap of the CDW[11]. The result is in figure 1.2.

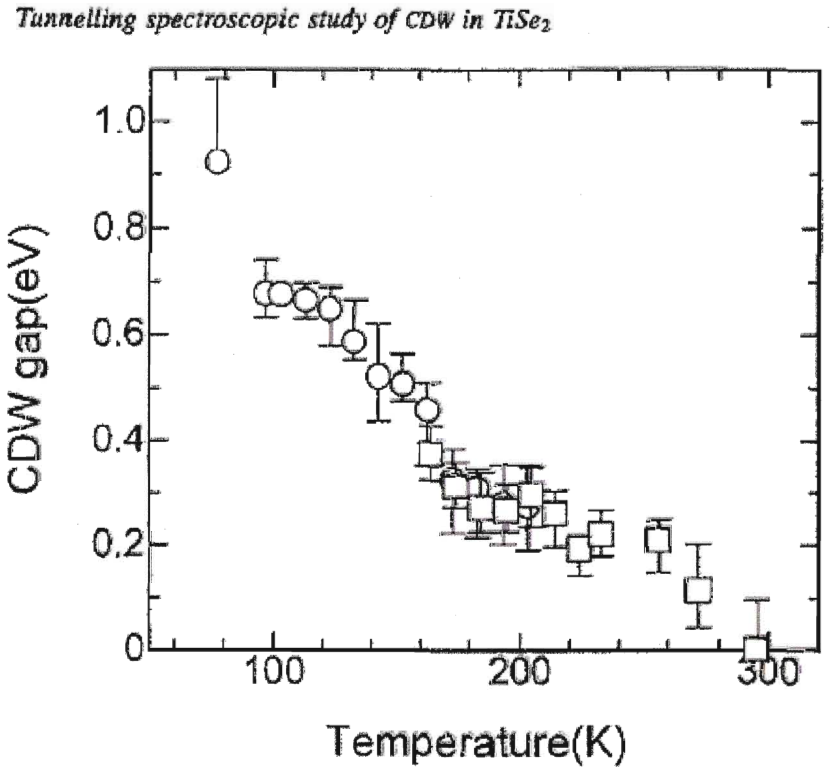

Figure 1.2: Experimental data of the CDW energy gap in $TiSe_2$[5]. The squares and the circles do not denote anything different between the two.

1.2.2 Cu_xTiSe_2

Morosan et al. sintered polycrystalline pellets of Cu_xTiSe_2 where the Cu is occupying layers inbetween the $TiSe_2$ layers[3]. The crystal structure they determined can be seen in figure 1.1. This intercalation of Cu into $TiSe_2$ expands the a and c lattice parameters of the crystal[3, 6]. The expansion relation is summarized in figure 1.3. The expansion of the a and c lattice parameters stops when x≈0.11 and this is believed to be the intercalation limit of Cu into $TiSe_2$[3]. The c-axis expansion is also observed when the parameter is measured on single crystals.[2]

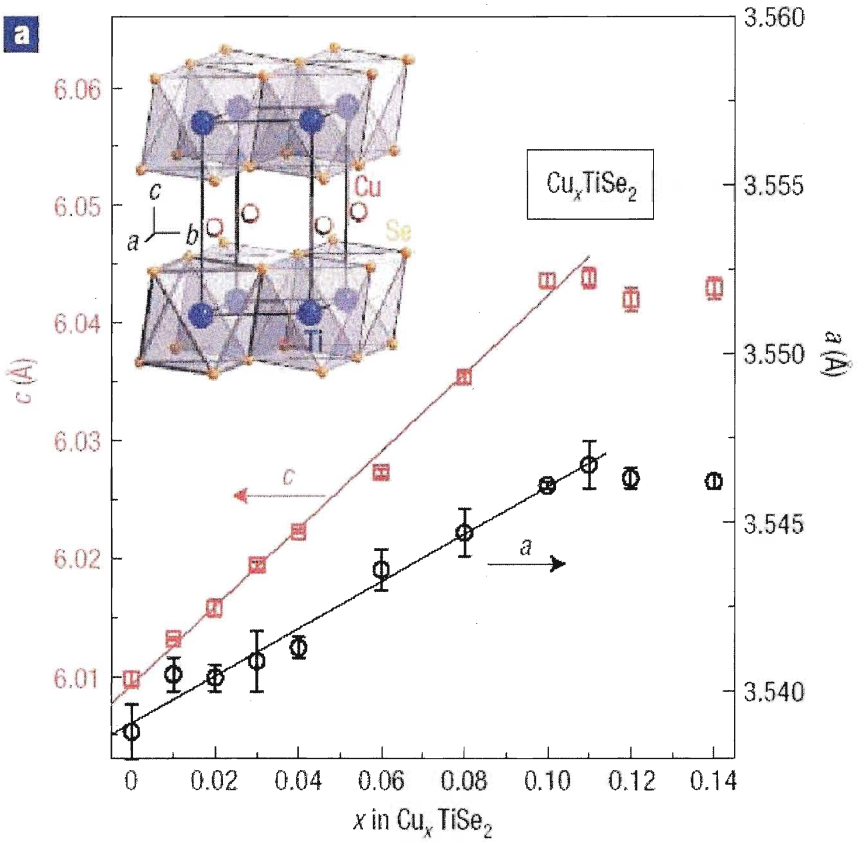

Figure 1.3: a and c lattice parameters vs Cu concentration[3].

Wu et al. measured the in plane thermopower for single crystals of Cu_xTiSe_2 for various Cu concentrations[2]. From their results, they concluded that the thermopower is large, the charge carriers are electrons, and the intercalation of Cu enhances the metallic behaviour of the material. The conclusion that the charge carriers are electrons is consistent with the studies on $TiSe_2$. Wu et al. also measured resistivity along the ab plane as well as through the c axis[2]. Their results

indicate that the charge transport mechanism is the same in both of these orientations.

Cu intercalation is also found to suppress the CDW state[3]. However, suppression of the CDW state is observed in $TiSe_2$ when there is excess Ti[10] and when there is doping with other transition metals[4]. Cu intercalation into this system is unique because with optimum intercalation a superconducting state emerges[3]. No superconducting state has been observed by doping with other 3d transition metals[2].

Morosan et al. also measured the temperature dependence of magnetic susceptibility and resistivity on their polycrystalline pellets of various Cu concentrations[3]. The magnetic susceptibility and the resistivity measurements are in figure 1.4 and figure 1.5, respectively. They determined through figure 1.4 that the CDW phased

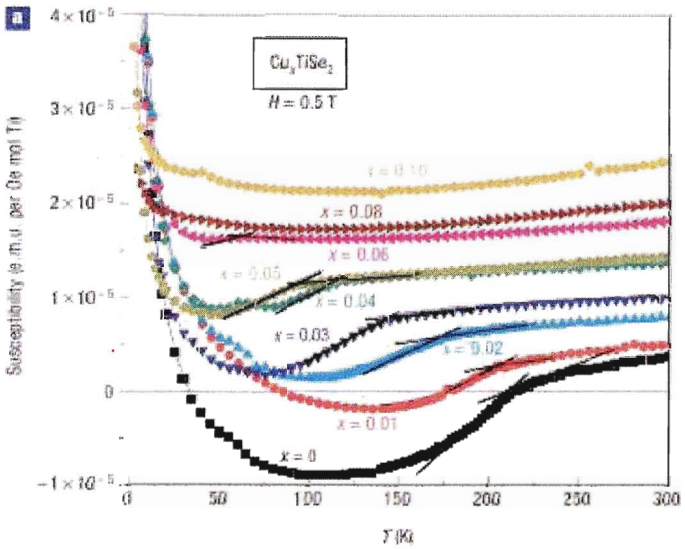

Figure 1.4: Susceptibility of Cu_xTiSe_2[3].

out completely when x≈0.06. Also, the effects from the CDW diminishes as the Cu concentration increases. Figure 1.5 was found to be consistant with these conclusions[3].

Their results for lower temperatures on the magnetization and the resistivity can be seen in figure 1.6 and figure 1.7, respectively. They noticed that a SC state emerges when x>0.04 in a system that can reach a temperature as low as 0.4K[3]. The SC state optimizes when x≈0.08 giving a onset temperature of 4.15 K. This is consistent with single crystals, where the maximum onset temperature of 4.13 K is found when the Cu concentration is 0.08[2]. The electronic state diagram for various Cu concentrations derived from analysis of the polycrystalline growth is seen

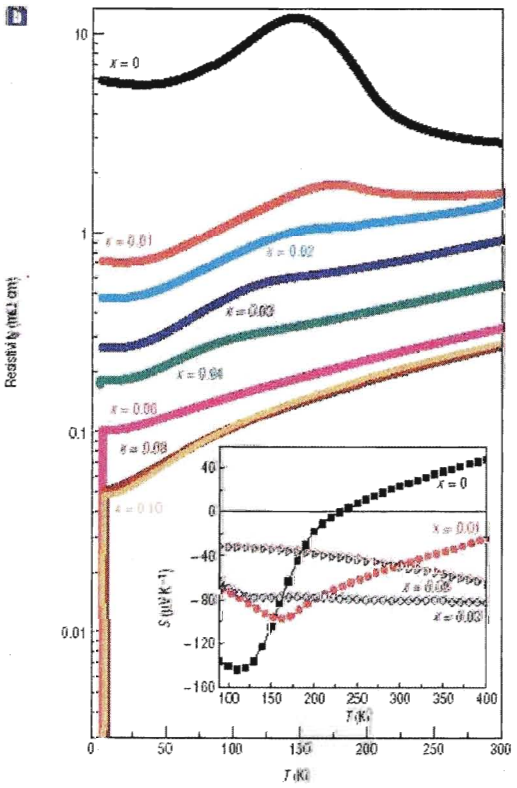

Figure 1.5: Resistivity on polycrystalline pellets of Cu_xTiSe_2[3].

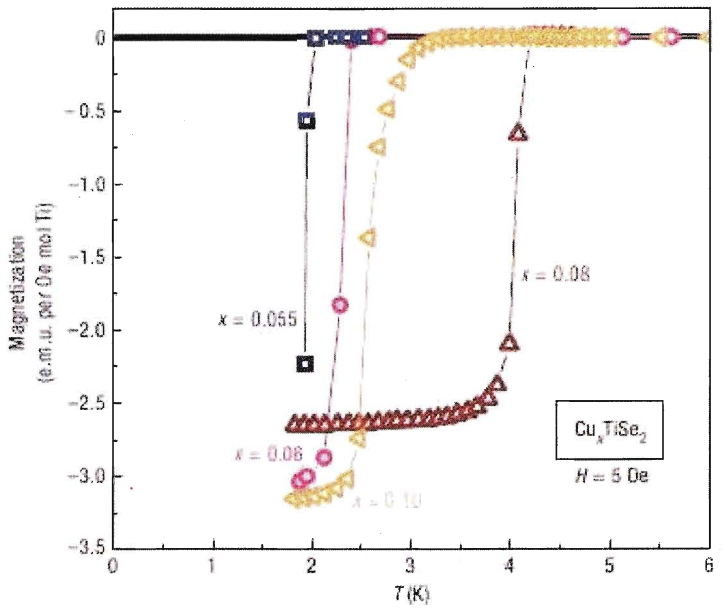

Figure 1.6: Magnetization of Cu_xTiSe_2 at low temperature[3].

in figure 1.8.

It is observed that doping with Cu supresses the CDW. However, Morosan et al. were able to perform electron diffraction on polycrystal they grown, and concluded that the CDW wavevector is not affected by the Cu doping[3]. Wu et al. feel that the supression of the CDW could be caused by the structural change that Cu induces to the crystal structure[2]. Zhao et al. have another explanation for the supression of the CDW. By using photoemission spectroscopy they argue that the CDW is suppressed because the Cu raises the chemical potential and therefore weakens the electron hole coupling, which supresses and destroys the CDW[4]. Barath et al. performed temperature and Cu dependant Raman scattering studies on the CDW. In their work they found that the temperature dependence on the CDW has the same decay as the Cu concentration dependence on the CDW[6].

Li et al. measured the thermal conductivity in various magnetic fields and found the material has only one superconducting energy gap[1]. Morosan et al. also measured the magnetization with respect to magnetic fields for various temperatures on poly crystals[3]. From this they found the superconductivity is of type-II and the critical magnetic field values follow the theory for conventional superconductors. Also. by measuring the specific heat, they found that the normal state electronic contribution to the specific heat has a value of $4.3\frac{mJ}{molK^2}$[3], which is denoted with γ. They were able to determine by using this value and the transition temperature,

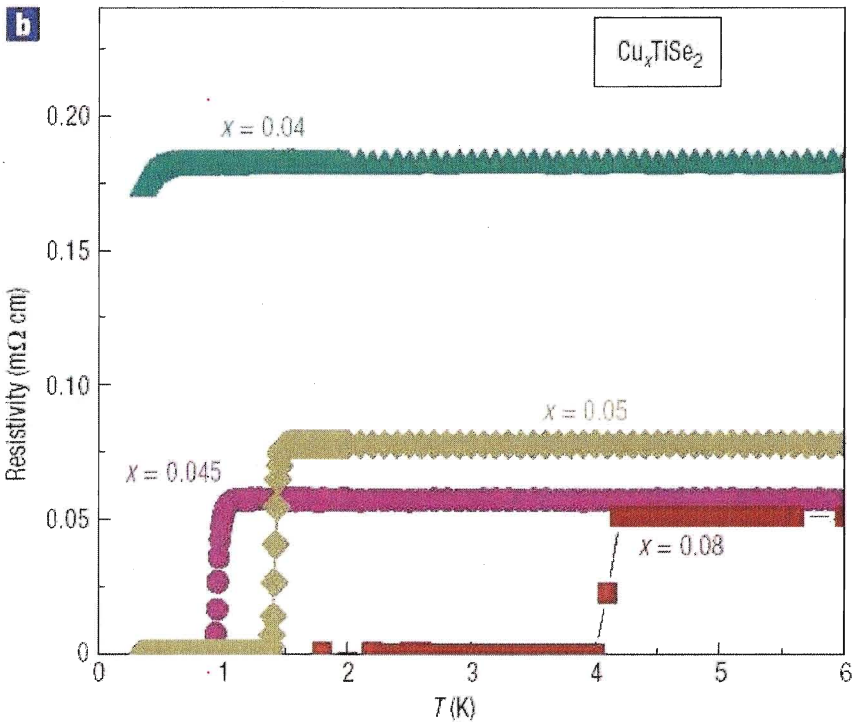

Figure 1.7: Resistivity on polycrystalline pellets of Cu_xTiSe_2 at low temperature[3].

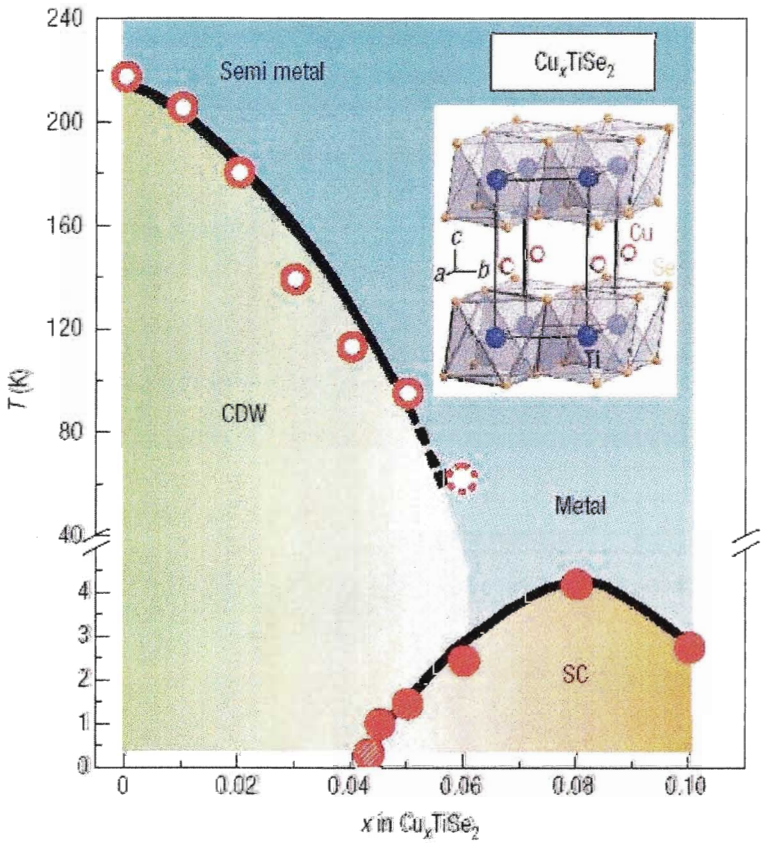

Figure 1.8: Electronic phase diagram of Cu_xTiSe_2[3].

that, the material is expected to be a conventional superconductor[3]. Also, the theory for conventional superconductivity predicts that

$$\frac{\Delta C_e(T_c)}{\gamma T_c} = 1.49 \tag{1.1}$$

where T_c is the transition temperature into the superconducting state,and for their calculation they found it to have a value of 1.68, which they feel is acceptably close[3]. Experiments from Li et al. agree with the material being a conventional superconductor[1]. They concluded this by measuring the thermal conductivity on the ab plane of single crystals and found that there was absence of a residual linear term as temperature approached zero. They believe this is strong evidence that the material is a conventional superconductor[1].

Relations of the SC state with respect to Cu doping are better understood by re-examining figure 1.4. Morosan et al. noticed that by introducing more Cu, the susceptibility at 300 K increases[3]. They believe this can be explained because by adding more Cu, more carriers are introduced into the conduction band of $TiSe_2$. This leads to the density of states increasing since there are more carriers, and thus the Pauli paramagnetism increases. Morosan et al. also observed an enhancement in the density of states in their specific heat curves[3]. Therefore, these two independent measurements enhance this arguement. Zhao et al. also believe the superconductivity is a product from the enhancement in the density of states[4]. Zhao et al. also remarked that the decrease in the SC state after the optimum SC state is possibly caused by the strong inelastic electron scattering[4].

1.3 Motivation and Goal

It is evident that some properties stated about this material are inconsistent. This statement raises alarm because it may be an indication that other conclusions about the material's properties may not be able to explain all other experimental results. Therefore, it is crucial to attempt various experiments to verify if the properties stated already are consistant with other experimental results.

The superconducting energy gap has not been measured on this material. Therefore a measurement of the superconducting energy gap would be an excellent independent study that could be used to verify some properities of the material. Point contact spectroscopy (PCS) is the experimental procedure that measures the superconducting energy gap.

Therefore, in this thesis, crystals of Cu_xTiSe_2 shall be grown and PCS shall be employed on them. By comparing the data to the theories for PCS, the superconducting energy gap can be extracted. These values can be used to check if the material has a single SC energy gap and to check if there is an agreement with what

is predicted for a conventional superconductor.

Chapter 2

Theoretical Background

2.1 Magnetism in Materials

Magnetism in materials comes from the combination of the magnetic moments from the spin of electrons, the orbit of the electrons, and the change in orbital momentum when a magnetic field is applied. Nuclear magnetic moments also contribute but these moments are on the order of 1000 times weaker than the contribution from the electrons. Therefore, the nuclear magnetic moment contributions are neglected. The spin and the orbital moment of electrons have the ability to generate paramagnetism in materials, which contributes positively to the susceptibility of the material. The change in orbital moment creates diamagnetism. Diamagnetism contributes negatively to the overall susceptibility.

The magnetic susceptibility per unit volume is defined as:

$$\chi = \frac{\mu_0 M}{B} \tag{2.1}$$

where μ_0 is the permeability of free space, M is the magnetization per unit volume, and B is the applied magnetic field. Sometimes the susceptibility is reported per unit mole or per unit gram. The magnetization per unit volume is defined as:

$$M = \frac{m}{V} \tag{2.2}$$

where m is the magnetic moment, and V is the volume.

2.1.1 Langevin Diamagnetism

Diamagnetism occurs in all materials when placed in a magnetic field. When a magetic field is applied, the material creates a magnetic moment to counter the magnetic field. This magnetic moment exists until the field is removed.

For an atom, the classical derivation of the diamagnetic component of magnetic susceptibility shows that:

$$\chi = -\frac{\mu_0 N Z e^2}{6m} < r^2 > \tag{2.3}$$

where N is the number of atoms per volume, Z is the atomic number, e is the charge

of an electron, m is the mass of an electron, and $< r^2 >$ is the average of the radius squared. A quantum approach to describe the diamagnetic contribution has reproduced this classical result.

2.1.2 Paramagnetism

Paramagnetism is seen in a variety scenarios, all in which the total angular momentum does not equal zero. Therefore, paramagetic properties arise when there are an odd number of electrons in atoms or molecules. However, it does occur in some materials with even numbers of electrons, such as molecular oxygen. In this case the total angular momentum still does not equal zero. For the same reasons, paramagnetism is also seen in metals and when free atoms or ions have a partly filled inner shell.

In the Langevin-Curie derivation of paramagnetism, it can be shown that as mB$<<$ k_BT the susceptibility takes the form:

$$\chi = \frac{C}{T} \tag{2.4}$$

where C is the Curie constant, T is the temperature, and k_B is the Boltzmann constant. Therefore in this limit, the susceptibility is inversely proportional to temperature. This dependancy has been seen in experiment and is shown in figure 2.1.

It has been found that most nonferromagnetic metals have susceptibilities independent of temperature. Pauli found that application of the Fermi-Dirac distribution explained the temperature independence. The argument for these materials is that conduction electrons can not simply flip spins because there are electrons already occupying these states. There are only a small fraction of electrons that can flip their spins and they have an energy in the range of k_BT. After this correction, the theory for the susceptibility could be expressed approximately as:

$$\chi \approx \frac{Nm^2}{k_B T_F} \tag{2.5}$$

Thus, in this situation, the susceptibility is temperature independent.

For further information on magnetism in materials refer to [15].

2.2 Charge Density Waves

When cooling down certain metallic materials the material will enter into a CDW state. The transition into the CDW state is called the Peierls transition and

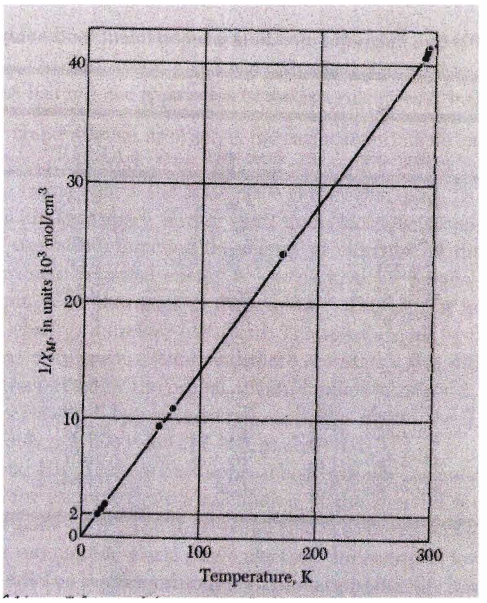

Figure 2.1: Temperature dependence on susceptibility for galidium salt. The straight line is the Curie law[15].

is a second order phase transition. The CDW state is due to a change in the position of the lattice atoms and a change in the electron density. This is demonstrated in figure 2.2. The change in the atomic positioning is very small, where the change in positions is on the order of a one percent difference. The electronic displacement varies and tends to be greater than the atomic displacement. Peierls pointed out that a modification in the lattice atoms produces an energy gap (2Δ). The energy gap is caused by an instability in the Fermi surface involving an electron-phonon interaction creating an energy gap at $k=\pm k_F$. Opening of an energy gap reduces the total electronic energy. The energy it takes to move the atoms is less than the gain in conduction electron energy. Therefore this system is favourable. As temperature is increased, the energy of the CDW system is reduced by thermal excitations across the gap.

Modulations in the CDW have a wavelength of:

$$\lambda_c = \frac{\pi}{k_f} \tag{2.6}$$

where λ_c is the wavelength of the charge density wave. λ_c is expected to be an integer multiple of the wavelength of the lattice, and if it is not it is usually caused by impurities in the material.

CDWs have weakly coupled molecular chains, where highly delocalized electrons

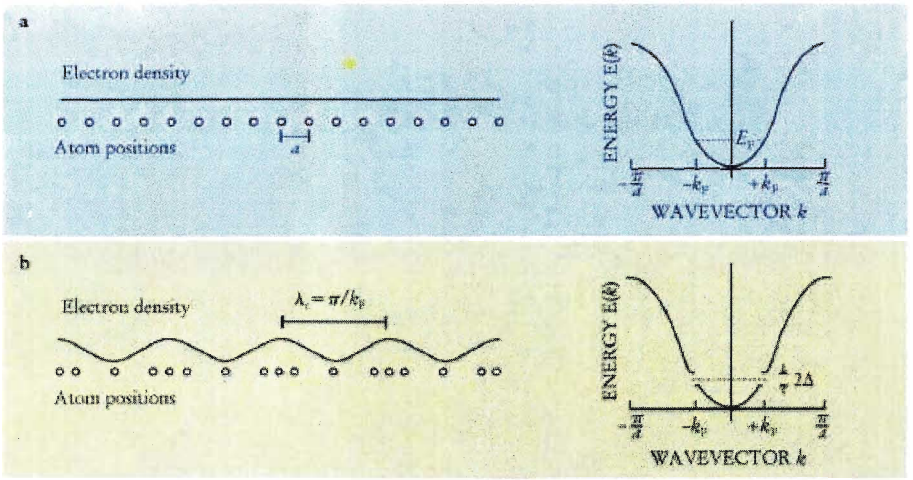

Figure 2.2: Diagram of the change in electron and atom position in a CDW. a is for a metal and b is for a CDW[16].

move easily along the chain. Thus, CDWs have anisotropic properties. When CDW materials are not in the CDW state, they are anisotropic metals. The resistivity along the chains are usually 1-3 times smaller than the resistivity perpendicular to the chains. Additionally, the resistivity along the chains is typically 3 times smaller than that of copper.

When CDW materials transition into a CDW state, there are lots of quasi-particles being excited across the energy gap. Thus, the resistivity is fairly linear with respect to temperature. As the temperature is decreased further, non-linear effects become dominant because the single particles do not have the energy to overcome the energy gap. It has also been noted in some CDWs that a change in the electric field by a few percent can switch the material from metallic state to an insulating state with the resistivity changing by more than 10 orders of magnitude.

CDWs are like SCs, they both have collective charge transport. The difference is that the resistance for a CDW is not zero, which is the case for a SC. Various mechanisms damp the motion of the charge and this gives the difference between the two. Lots of materials have CDW states but only a small fraction of them show collective charge transport. The reason why some materials do not show collective charge transport could be due to pinning effects to the lattice being too strong. For materials that do show collective charge transport, when an electric field is applied, the CDW 'slides' relative to the lattice. The lattice atoms oscillate back and forth producing a traveling potential and electrons move with this potential producing a current. The sliding occurs when the electric field is above a certain threshold. Therefore, if a DC electrical potential is applied across the material, the CDW will

give an AC current.

CDWs are rich in dynamical behaviour due to the nonlinear characteristics and the uncommon electronic properties. CDWs are also known for having giant dielectric constants and unusual elastic properties. To learn more about these properties or more about properties of CDWs that were not discussed in this section, refer to [16] and [17].

2.3 Superconductivity

In 1911, Onnes was the first person to discover superconductivity existed in certain materials. He noticed that upon cooling certain materials towards liquid He temperatures, there was an abrupt change from finite to zero resistivity. This zero resistivity state is denoted as a SC state. In 1933, a strong diamagnetic susceptibility was found in superconductors. In fact, the magnetization was of equal magnitude to the magnetic field applied. Thus, SCs are called perfect diamagnets. It was found that a thin layer near the surface is producing this diamagnetic moment, which in turn prevents magnetic flux from entering inside the SC material.

This perfect diamagnetic property in superconductors only exists for magnetic fields up to a certain critical magnetic field. There are two things that can happen to superconductors as the magnetic field is increased beyond a critical point:

1. **In Type I superconductors** - The superconducting state destroyed.

2. **In Type II superconductors** - The sample enters an intermediate state (vortex state) where some of the field penetrates through the sample but the rest of the sample repels the field. The strength of the repulsion decreases as the magnetic field is increased since the penetration grows larger. Eventually all of the superconducting state is destroyed as the penetration grows as large as the material. This is when the magnetic field reaches a second critical point.

By decreasing the field below the critical points, the effects are undone, and the SC state will exist again for both type I and type II superconductors. Type I superconductors generally have a lower critical field than type II.

Specific heat measurements of superconductors show that there is usually a energy gap. Measurements of entropy show that the system becomes more ordered. Additionally, it was found that superconductors have an isotope effect. As the mass of an isotope increases, the transition temperature to enter the superconducting state for that material decreases. These properties along with others were explained in the theory of superconductivity (BCS Theory)[18].

In BCS theory, superconductivity is explained through an energy gap model. The energy gap (2Δ) is related to the transition temperture into the superconducting

state (T_c) as follows:

$$\Delta_0 = \frac{3.5}{2} k_B T_c \tag{2.7}$$

where k_B is Boltzmann's constant. Near T_c, Δ may be expressed as:

$$\Delta = 3.2 k_B T_c \sqrt{1 - \frac{T}{T_c}} \tag{2.8}$$

where T is the temperature. The temperature dependence of Δ was derived and the equation may be re-expressed and written in the following form:

$$ln\frac{\Delta(T)}{\Delta(0)} = -2\int_0^\infty \frac{dE}{\sqrt{E^2+\Delta^2}} f(\frac{\sqrt{E^2+\Delta^2}}{k_B T}) \tag{2.9}$$

where f is the Fermi-Dirac distribution. The plot for equation 2.9 can be found in figure 2.3.

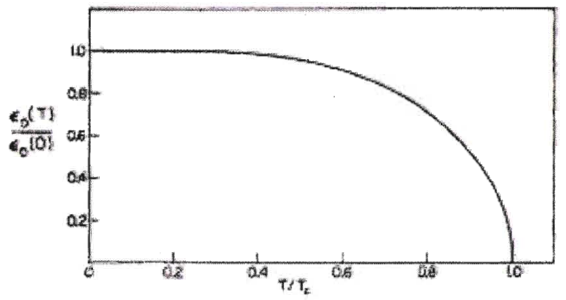

Figure 2.3: Theoretical data of the SC energy gap with normalized axes. T is the temperature, T_c is the superconducting transition temperature, e_0 is half of the superconducting energy gap[18].

BCS theory discusses that electrons pair together (Cooper pairs), with the mediation of phonons, to form a less energetic state. Some or sometimes all of the conduction electrons participate in this state. Thus, an energy gap is created. This explains the specific heat curves found experimentally for SCs. Also, the isotope effect is explained because of the electron-phonon coupling. Different isotopes effect the phonons, thus effecting the superconducting properties. This is why different isotopes show different transition temperatures. Finally, entropy measurements were explained because of Cooper pairs forming. The Cooper pairs are a more ordered state, and this is why the experimental measured entropy is consistant.

When a material is going from a normal to superconducting state, the process is reversible. The transition is a second order phase transition. It should also be

noted that the Meissner effect is a product of the energy gap. BCS theory was able to explain and relate these physical properties , as well as others. However, there have been other materials found that have a SC state that do not agree with BCS theory. These materials have been denoted as unconventional SCs and KOs_2O_6 is an example of one[19].

For more information on superconductivity or superconductors please refer to [15, 18, 19, 20, 21].

2.4 Point Contact Spectroscopy

Point Contact Spectroscopy (PCS) is applicable for determining various physical properties but is dependant on the two materials being connected through a point contact (PC). This summary is designed to outline one particular scenario of PCS. Here within this summary, it is bound to when:

1. The PC is made between a metal and a superconductor (N-S interface).

2. The PC allows the electrons to remain in a region where Joule heating does not destroy the superconductivity. The optimum region is when the mean free path of the electrons is larger than the diameter of the contact (ballistic regime).

3. The analysis of the current with respect to electrical potential (IV) characteristics are used to determine the superconducting energy gap.

Although this type of contact can be used to extract other physical properties, this summary will stick within the realm of the theory that pertains to this project.

In 1982 Blonder, Tinkham, and Klapwijk wrote a theoretical paper (BTK theory) to describe the physical nature when a superconductor and a metal are connected through a point contact[22]. BTK theory is based off of a one dimensional metal to semiconductor model which is used to qualify the allowed transitions at the interface. The allowed transitions were quantified by utilizing Bogoliubov equations. In addition, the theory also used an Andreev reflection model and omitted Josephson effects in their derivations. Other theories have been able to determine the probabilities of transitions, but BTK theory has more physical significance because it was able to be extended to theoretically quantify IV characteristics.

The possible transitions at the interface, denoted with A, B, C, and D, can be seen in figure 2.4. The probabilities of each transition is reprinted and can be seen in table 2.1. Z is the barrier potential, which comes from the physical contact that is made. In BTK theory the IV characteristics were equated, and the current was

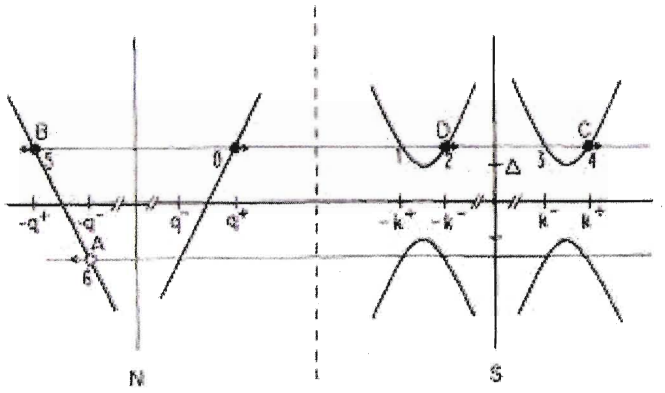

Figure 2.4: Metal to superconductor interface diagram. 0 represents an electron on the metal side traveling towards the interface. A represents Andreev reflection, B represents a reflection, and C and D represent transitions of a single electron[22].

determined to be:

$$I = AJ = 2 * N(0)ev_F A \int_{-\infty}^{\infty} [f_{\rightarrow}(E) - f_{\leftarrow}(E)]dE \tag{2.10}$$

where A is an effective cross sectional area of the contact, J is the current density, N is the density of states, e is the charge of an electron, v_F is the Fermi velocity, f is the Fermi-Dirac distribution, and 2 is due to the electron spin. BTK theory shows that

$$f_{\rightarrow}(E) = f_0(E - eV) \tag{2.11}$$

and,

$$f_{\leftarrow}(E) = A(E)[1 - f_{\rightarrow}(-E)] + B(E)f_{\rightarrow}(E) + [C(E) + D(E)]f_0(E) \tag{2.12}$$

where V is the electrical potential. By using the relation that the sum of all probabilities must be equal to 1 and other relations, it was shown that equation 2.10 can be written as

$$I = 2 * N(0)ev_F A \int_{-\infty}^{\infty} [f_0(E - eV) - f_0(E)][1 + A(E) - B(E)]dE \tag{2.13}$$

In BTK theory, equation 2.13 was numerically solved and plotted as well as the conductance was plotted. Normalized current and conductance curves can be seen in figure 2.5 and figure 2.6, respectively. It is clear from figure 2.6 that Δ can

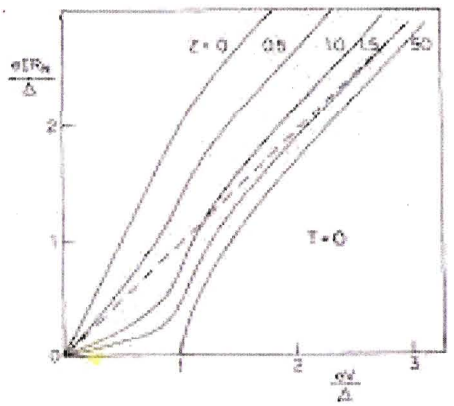

Figure 2.5: Theoretical IV curve from BTK theory[22].

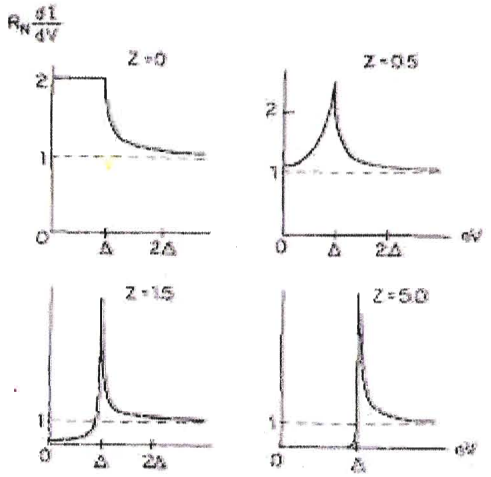

Figure 2.6: Theoretical conductivity curve from BTK theory. Reprint[22].

Table 2.1: Probability of N-S interface transitions.[22] Z is the barrier potential, u_0, v_0, and γ are parameters described within BTK theory, Δ is half of the superconducting energy gap of the material, and E is a parameter of integration.

	A	B	C	D
Normal State	0	$\frac{Z^2}{1+Z^2}$	$\frac{1}{1+Z^2}$	0
$E < \Delta$	$\frac{\Delta^2}{E^2+(\Delta^2-E^2)(1+2Z^2)^2}$	1-A	0	0
$E > \Delta$	$\frac{u_0^2 v_0^2}{\gamma^2}$	$\frac{(u_0^2-v_0^2)^2 Z^2(1+Z^2)}{\gamma^2}$	$\frac{u_0^2(u_0^2-v_0^2)(1+Z^2)}{\gamma^2}$	$\frac{v_0^2(u_0^2-v_0^2)Z^2}{\gamma^2}$
$E < \Delta$ (Z=0)	1	0	0	0
$E > \Delta$ (Z=0)	$\frac{v_0^2}{u_0^2}$	0	1-A	0
$E < \Delta$ (large Z)	$\frac{\Delta^2}{4Z^2(\Delta^2-E^2)}$	1-A	0	0
$E > \Delta$ (large Z)	$\frac{u_0^2 v_0^2}{Z^4(u_0^2-v_0^2)^2}$	1-$\frac{1}{Z^2(u_0^2-v_0^2)}$	$\frac{u_0^2}{Z^2(u_0^2-v_0^2)}$	$\frac{v_0^2}{Z^2(u_0^2-v_0^2)}$

easily be determined by visually inspecting the conductivity curves with respect to the electrical potential.

BTK theory is based on the fact that the quasi particles have an infinite lifetime. If the contact is not in the ballistic regime this would not be the case, and scattering would occur, causing quasiparticle lifetime effects. As long as the scattering is not too large to cause Joule heating, theory has been derived to take this scattering into account. Dynes et. al. in 1978, included lifetime effects for PCS[23]. Plecenik et. al. took a formula similar to Dynes and spelt out the modifications that would be needed to modify BTK theory[24]. The formula similar to Dynes was:

$$N(E,\Gamma) = Re\left(\frac{E+i\Gamma}{\sqrt{(E+i\Gamma)^2-\Delta^2}}\right) \tag{2.14}$$

where N is the density of states, Δ is half of the superconducting energy gap, and E is a paramater used for integration. Mitrovic and Rozema argued that the imaginary part of E can not be physically justified[25]. However, they argue that there is physical significance when Δ has an imaginary part rather than E, which relates to the quasiparticle lifetime. They also went on to show that if the imaginary term is small relative to Δ, both theories will correlate.

For more information refer to[22, 23, 24, 25, 26]

2.4.1 Bogoliubov Equations

The Bogoliubov equations are an approximation to determine the ground-state wave function and ground-state energy of a quantum many-body system. The equations are able to include the effects of the superconducting pairing potential as well as the ordinary scalar potential[20].

2.4.2 Andreev Reflection

When an electron is traveling from a metal to a superconductor, and the electron has less energy than Δ, the electron must either reflect or form a Cooper paper if it were to travel across the interface. For a Cooper pair to form, another electron must couple to the traveling electron. Due to this additional electron a hole is reflected at the interface. Andreev reflection denotes the hole being reflected at the interface, which generates a doubling of current. When electrons have more energy than Δ, Andreev reflection still exists but single particles can now cross the interface too.

For more information please refer to [26].

2.4.3 Josephson Effects

Josephson effects occur when there is a SC-Insulator-SC interface. If no voltage is applied across this interface, naturally a DC current will be observed. This DC current depends on the phase difference between the two superconductors as well as the thickness of the insulator. If a DC electrical potential is applied across the interface an AC current can be observed which oscillates proportional to the electrical potential. If two SC-Insulator-SC interfaces are placed in parallel and a magnetic field is varied perpendicular to the interfaces, an interference pattern will previal in the electrical potential across the parallel interfaces.

For further information please refer to [15].

Chapter 3

Experimental Techniques

3.1 Single Crystalline Growth

Superconducting single crystals need to be grown. Fortunately, Morosan et al. described a method to produce superconducting single crystals where the composition produced $Cu_{0.07}TiSe_2$[5]. Therefore, the procedure for growing single crystals coincided with this one. The steps that Morosan et al. took to grow single crystal can be summarized as follows:

1. Create crystals of $TiSe_2$. This is accomplished by first mixing stoichiometric amounts of Ti and Se in an evacuated silica tube. Then heat the tube to a temperature of approximately 650°C for about 10 hours. The ends result is the $TiSe_2$ crystals.

2. Use the $TiSe_2$ and introduce Cu to the system to produce the desired single crystals. This was done by adding $CuCl_2$ to the $TiSe_2$ in a 1:10 ratio in an evacuated silica tube. The dimensions of the silica tube that housed the material was 150 mm long and 12 mm in diameter in their case. They took this ampule and placed it into a temperature gradient with a hot end temperature of 650°C and the cool end temperature of 550°C. They noted that the reactants should be placed on the hot end and after two weeks, the crystals should be acquired.

For the single crystal growths the amount of $CuCl_2$ was varied to try and create various compositions of Cu_xTiSe_2. Also, it is crucial to minimize impurities. Therefore, the reactants were to be exposed only to a nitrogen rich atmosphere or no atmosphere at all.

All growths were started by mixing the stoichiometric amounts of the Ti and Se with 5 percent excess Se into a quartz tube. Excess Se is needed to help ensure the stoichiometry is correct[10]. The quartz tube was pumped on using a turbomolecular pump, to create high vacuum. Once the pressure was at an acceptable level, approximately less than 10μTorr, the quartz tube was sealed. The sealing was done by using combustion from natural gas mixed with oxygen to get the desired heat to work the quartz. The seal needed to be done in a short amount of time to prevent loss of product due to heat. After the seal was made, the tube was placed in

an oven. The oven was brought up steadily from room temperature to the desired temperature of 650°C over a time span of 12 hours. The oven remained at this temperature for 24 hours. After this, the temperature of the oven was brought back to room temperature over another 12 hours. This should have produced the $TiSe_2$ needed for the second step.

The second step was started by breaking open the quartz tube to get the $TiSe_2$. The material was then mixed in desired proportions with $CuCl_2$ into another quartz tube. A vacuum was created in the tube, and it was then sealed in the same manor as discussed in the previous step. The tube was then placed inside an oven. From room temperature, the oven temperature was increased steadily over a 12 hour span to the desired temperature gradient. The reactants were in the hotter side of the gradient. The oven stayed at this temperature for 14 days and then it was brought back down steadily to room temperature over 12 hours.

3.2 Poly Crystalline Growth

A method by Morosan et al. described how poly crystalline pellets of Cu_xTiSe_2 were yield, where x was between 0 and 0.14[3]. Therefore the method attempted for growing poly crystals coincided with this method. The steps they took to grow their poly crystals can be summarized as follows:

1. Create poly crystals of Cu_xTiSe_2. This is done by mixing stoichiometric amounts of elemental Ti, Se and Cu into an evacuated silica ampule and heating the ampule from room temperature to 350°C in one hour. It is then heated further by increasing the heat 50°C/hour until 650°C is reached. Once at this temperature, the oven stays at this temperature for another 20 hours. This produces the Cu_xTiSe_2.

2. Press the Cu_xTiSe_2 into pellets and anneal them to improve homogeneity. This was done by taking the powders and pressing them into pellets. After, the pellets were placed in a vacuum. In this vacuum, they were annealed at 650°C for 50 hours. The final products were noted to be purple-grey pellets of Cu_xTiSe_2.

For the polycrystalline growths of Cu_xTiSe_2, the amount of Cu was varied to try and create various compositions. Steps were taken to minimize impurities, which followed the protocol discussed in single crystalline growths. There was one exception to this repeat of protocol; when pressing pellets the materials had to be introduced to normal atmosphere and could not be kept in a nitrogen rich environment.

All growths were started by mixing the stoichiometric amounts of Ti, Se and Cu into a quartz tube. A vacuum was created on the tube and the tube was sealed, as

described in the single crystalline growth. The quartz tube was placed in an oven where the oven was brought up steadily to the desired temperature of 650°C from room temperature over 12 hours. The oven was left at the temperature for 20 hours and then steadily brought back down to room temperature over another 12 hours.

The second step was followed by breaking open the quartz tube to get the product out. The product was then placed in a drybox to be ground down into a fine powder by using a mortar and pestle. The fine powder was then pressed into pellets of either 5mm or 13mm diameter. The pellets were then placed into a quartz tube which was pumped on with a turbomolecular pump to create high vacuum. While the pump was pumping, the tube was then placed inside an oven where it was heated up steadily over 12 hours. The oven stayed at this temperature for 50 hours and then it was brought back down steadily to room temperature over 12 hours.

3.3 Energy Dispersive Spectroscopy (EDS)

Energy dispersive spectroscopy (EDS) works as follows: Electrons of high energy are fired at a sample. An electron within the sample is freed from its orbit and leaves a hole. Another electron in a higher orbit, releases energy to place itself in the hole that was created. The releases of energy are dependant on the atoms within the sample since the atoms have unique and discrete orbit levels. Thus, the energy releases from the samples depend on what atoms are in the sample. Also, the frequency of the releases is related to the concentration of atoms in the material. The energy releases are measured by a detector counting the amount of energy releases there are at a specific energies. Therefore, the count versus energy level can be used for detection of the atoms in the sample and composition of the sample. Due to the detectors used, there are some atoms that can not be detected. Commonly, the detector for EDS can not detect atoms that have an atomic number less than or equal to Na.

All EDS work was done either by Glenda Hooper at Brock University or by the Max-Planck institute in Germany.

For more information on EDS refer to [27].

3.4 X-ray Diffraction

Constructive interference for three dimensional periodic crystal structures follows Braggs law, which can be stated as:

$$2dsin(\theta) = n\lambda \tag{3.1}$$

where n is an integer denoting the order, θ is the angle between the monochromatic wave and the surface of the material, λ is the monochromatic wavelength, and d is the inter-atomic spacing. d varies depending on the type and sizes of the crystal structure.

This formulation can be used to determine the crystal structure as well as the lattice parameters of a crystal if an interference pattern is measured with respect to θ. Since the spacing in crystal structures is very small, in order for diffraction to occur the wavelength must be small also. X-ray wavelengths are small enough to extract interference patterns for crystal structures.

X-ray equipment generates monochromatic x-rays, which are collimated and aimed at a desired sample. The sample is placed onto a mount with double sided tape. Pellets could be mounted, or single crystals could be ground down into a fine powder then mounted. X-ray experiments were only done on certain single crystal growths. Grinding down single crystals destroys them. Therefore, growths with few single crystals or high SC transition temperatures were exempt. X-ray diffraction performed on poly crystalline pellets did not have this problem because no material would be lost.

Once a sample is mounted, software drives the equipment to rotate the sample and the detector in sync to collect data. The collected data could then be analyzed. The peaks of the diffraction pattern were extracted from the graph using gaussian fits. The peaks as well as the known crystal structure type were then plugged into free software, DICVOL[28], which is used to calculate likely a and c lattice parameters. Additionally, DICVOL tells which Miller indices correspond to which peak.

To help with the analysis of the x-ray data, it was useful to compare the data to the x-ray data for $TiSe_2$. The x-ray data for $TiSe_2$ is well known and it can be found on the International Center for Diffraction Data[29]. The x-ray data for $TiSe_2$ is in Figure 3.1. Since the doping of copper is known to expand the a and c lattice parameters[3], the peaks will be slightly shifted compared to figure 3.1. Therefore, the Miller indices for each peak can be compared to the DICVOL output to check for consistency. If consistency exists then this gives reason to believe that the products are indeed Cu_xTiSe_2.

The a and c lattice parameters from DICVOL were then taken and compared to previously reported a and c lattice parameters. The a and c lattice parameters are proportional to the Cu content. Thus, it was used to try and determine the Cu content in the compounds measured. Morosan et al. also utilized this technique by comparing their a and c lattice parameters for their single crystal growths, to classify their copper contents[5].

For more information refer to [15].

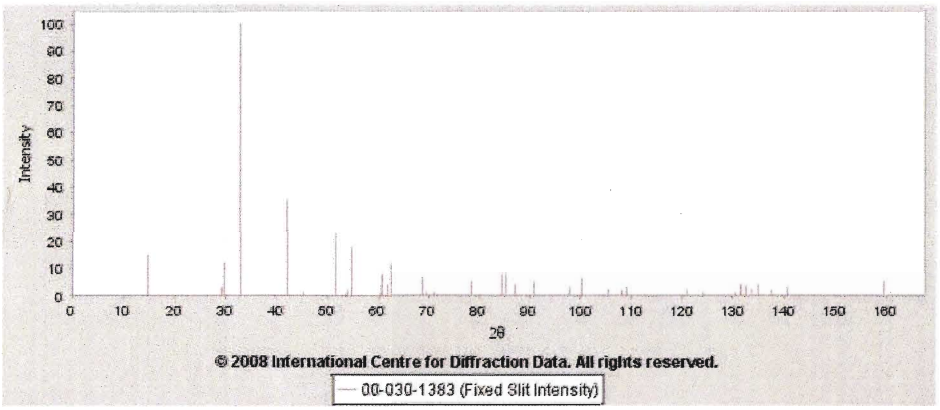

Figure 3.1: X-ray powder diffraction spectrum of $TiSe_2$[29].

3.5 Resistivity Measurements

All resistivity data was taken with respect to temperature. The resistivity experiment was setup in the sample chamber of a Magnetic Properties Measurement System (MPMS). This was done since the MPMS has quality temperature control as well as an ability to go down to 1.8 K.

The resistivity was measured using the Van Der Pauw technique[30]. The Van Der Pauw technique is able to measure resistivity of a uniformly thick material. The technique requires four electrical contacts to be made on the edge of the material. If that is too difficult, contacts could be placed on the surface as long as they are as far apart as possible and as close as possible to the edge of the material. The Van Der Pauw technique also requires that there are no holes through the material. Figure 3.2 shows a typical setup for this technique. In these experiments the electrical wires

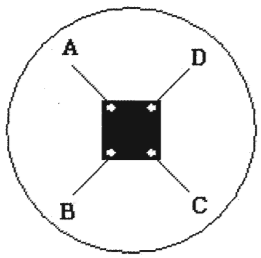

Figure 3.2: Setup for the ab-plane resistivity measurements. The black object is the sample. A, B, C, and D are electrical wires connecting to the sample.

were thin gold wires that were connected to the sample by using silver epoxy. The

other ends of the gold wires were soldered to other wires that connected the sample to the electrical system for the experiment.

The experiment works as follows: In order to calculate the resistivity a current must be applied, as seen in figure 3.2, from A to B and the electrical potential must be measured between C and D concurrently. The current is then reversed and the electrical potential is measured again. Using the two I and V parameters, two resistance could be calculated respectively. The average values of the resistance are taken. The values should essentially be the same. If they are not this could be a sign that there are poor electrical connections. This process is repeated again to get another average resistance by sending a current through B to C then measuring the electrical potential from A to D. The current is reversed like before, and the average resistance is determined again. Van Der Pauw has shown that these two average resistances must satisfy an equation [30]. This equation is:

$$e^{-\pi R_1 \frac{d}{\rho}} + e^{-\pi R_2 \frac{d}{\rho}} = 1 \tag{3.2}$$

where R_1 and R_2 are the average resistances, d is the thickness of the material, and ρ is the resistivity. Thus, the resistivity can be calculated.

Homemade software was used to control the experiment. Once all electrical connections were made, the software was able to switch the connections through a router. During execution, the software controlled the temperature of the sample space. Once the sample space was at the desired temperature, the software would then execute an algorithm to drive the current source and measure the various electrical potentials needed in order to calculate the resistivity. The software repeated this process for various temperatures.

3.6 Magnetic Susceptibility Measurements

Magnetic susceptibility measurements were all taken using a MPMS. All samples before being loaded into the MPMS were weighed in order to normalize the susceptibility values with respect to the weight of the material. Samples were inserted into the system by either being placed in a plastic capsule, which was suspended by a straw, or by placing the sample directly onto the straw. In the case where the sample was placed directly on the straw, a trace amount of silicon grease was used to hold the sample in place.

The magnetic field and temperature could be changed by using the computer that controlled system. All measurements were taken with fixed magnetic fields while the temperature was varied. The system measures magnetic moments. The magnetic susceptibility could then be determined from the magnetic moment by utilizing the weight of the sample and the strength of the magnetic field.

3.6.1 MPMS

The magnetic properties measurement system (MPMS) used to collect data, utilizes a DC SQUID (Superconducting QUantum Interference device). A SQUID is created from two superconductor-insulator-superconductor (SIS) interfaces being placed in parallel within a superconducting ring. The two interfaces utilize Josephson effects. If current is passed through the superconducting ring, and the voltage is measured while a magnetic field is applied perpendicular to the ring, an oscillating voltage will be measured. The oscillation properties depend on the current as well as the magnetic field.

In an MPMS system a specimen is moved up through pickup coils. The pickup coils get an induced potential from this motion. The induced potential is then sent through another coil, which induces a current into the DC SQUID. The MPMS is designed to take this input and accurately measure the magnetic moment from this action.

For a more detailed description refer to [31].

3.7 Point Contact Spectroscopy

To physically setup PCS, and to optimize the results a PC must be made where the contact allows the electrons to be in the ballistic regime. There are various ways to make the point contact. One of the new ways to make the point contact is to use silver paint. Silver paint is notorious for creating micro bridges much smaller than the contact made from the silver paint itself[32]. Thus, silver paint is excellent for trying to make contacts that keep the electrons in the ballistic regime. The physical wiring to a sample can be seen in figure 3.3. The current is passed from 1 through

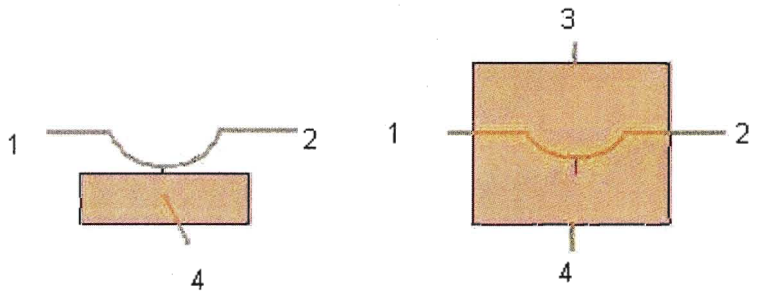

Figure 3.3: Physical wiring for PCS. The shaded area is the sample, and the numbers pertain to the ends of the wires.

3 and the potential difference is measured between 2 and 4. The point contact is

made between the wire connecting 1 and 2 and the middle of the sample, which is denoted in figure 3.3 with a small black line connecting the two.

A MPMS was exploited for its quality temperature control as well as its ability to go down to 1.8 K. Therefore, all measurements for PCS were done inside the sample chamber of a MPMS.

Homemade software was used to control the experiment after all the electrical connections were made and the sample was loaded into the MPMS. During execution, the software drove the MPMS to a specific temperature. The software would then execute an algorithm where the current would be varied and the potential difference would be measured. This was repeated at various currents to get IV characteristics.

Conductivity vs. electrical potential curves could be plotted using the data extracted from above. The energy gap could be determined directly from the these curves as long as the lifetime of the quasiparticles is infinite. In the non-infinite case a fit can be done to determine the superconducting energy gap.

The curves were fit to the theoretical equations that were derived by Plecenik et al.[24]. The Levenberg-Marquardt method was used in order to optimize the fitting parameters. The source code that was written to do the fits can be found in Appendix A.

The code generates the best fit by optimizing Δ, Z, Γ, and C, where C is a normalization for the theoretical data. Therefore, if the experimental data is not perfectly normalized, this parameter will optimize to correct it. By collecting many Δ's for different temperatures, they can be used into another fitting program.

The new fitting program is designed to use the Levenberg-Marquardt method to fit the data to what BCS theory predicts for various Δ's with respect to temperature. The source code for this program can be found in Appendix B. For the BCS fit, the Δ when the temperature is zero (Δ_0) is the parameter that is being optimized. As seen in equation 2.7, Δ_0 is related to the critical temperature. Therefore, this optimization is equivalent to optimizing the transition temperature. Fits can also be forced to a specific transition temperature. If there is strong confidence in the transition temperature, it is better to force the fit to the specific transition temperature and not allow the program to try to optimize it. This could be very useful, especially when trying to determine if a material is a conventional superconductor or not.

3.7.1 Point Contact Spectroscopy in Temperatures Below 1.8K

Equipment was designed to measure PCS below 1.8 K. The equipment was a removable modification to the MPMS. Rather than the system being cooled down

using helium gas by the reduction of pressure, He-3 was used instead.

3.7.2 Levenberg-Marquardt Method

Marquardt developed a method suggested by Levenberg to minimize the Merit function. The method was to utilize both the inverse Hessian method and the steepest descent method. The problem with the steepest descent method is that it has issues with knowing how long a slope will continue for. However, the inverse Hessian method can give insight into this. Thus, this is why a combination between the two is useful.

The Levenberg-Marquardt method has been designed to utilize the Hessian method when far away from a minima, and to weigh more heavily on the steepest slope method as the minima is approached. This method has been found to work well in practice, and is the standard for nonlinear least-squares routines[33].

The Merit function is the sum of squares between theoretical data and experimental data. The function is defined as:

$$\chi^2 = \sum_{i=1}^{N} \frac{y_i - y(x_i; \vec{a})}{\sigma_i} \tag{3.3}$$

where N is the number of data points, i denotes which data point, y_i is the experimental y data point, x_i is the experimental x data point, $y(x_i; \vec{a})$ is the theoretical function where $\vec{a}$ are the fitting parameters, and σ_i is the standard deviation of the data point. The method finds the minimum to this function by determining better fitting parameters. The better fitting parameters are found by solving:

$$\sum_{l=1}^{M} \alpha_{kl}\delta_{a_l} = \beta_k \tag{3.4}$$

where M is the number of fitting parameters. δ_{a_l} will tell the shift that should be applied on the fitting parameters to attempt to further reduce the Merit function. α_{kl} is computed by:

$$\alpha_{kl} = \sum_{i=1}^{N} \frac{1}{\sigma_i^2} \frac{\partial y(x_i; \vec{a})}{\partial a_k} \frac{\partial y(x_i; \vec{a})}{\partial a_l} \tag{3.5}$$

except when k=l, α_{kl} is the same as seen in equation 3.5 except it is multiplied by $(1+\lambda)$, where λ is a parameter for the fitting method. β_{kl} is computed by:

$$\beta_{kl} = -\frac{1}{2}\frac{\partial \chi^2}{\partial a_k} \tag{3.6}$$

In practice, to use this method, initial guesses are attempted and the Merit

function is computed. λ can be set to any value but 0.001 is a good starting value. δ_{a_l} is then determined, and the new parameters are attempted when computing the Merit function. If the new Merit function is smaller in value than the old, the process is repeated by using the new parameters and by increasing λ by a factor of 10. If not, λ is decreased by a factor of 10 and the old fitting parameters are attempted again. This whole process keeps getting repeated until the Merit function's change becomes really small in comparison to the value of the Merit function. At this point the minimum is essentially reached.

For further information refer to [33].

Chapter 4

Sample Preparation

4.1 Initial Growths and Characterization

Three growths were attempted with 0.2, 0.3, and 0.4 ratios of $CuCl_2$ to $TiSe_2$. The $CuCl_2$ content was doubled tripled and quadrupled since previous attempts of a 0.1 ratio failed to show superconductivity above 1.8 K and further analysis seemed to point to a lack of Cu. There were difficulties during the 0.2 growth with measuring the amount of $CuCl_2$, so this ratio could not be gauranteed. At the end of each growth, product could be seen in the cold and hot zone of the ampule. The desired product was expected to be in the hot zone[5].

Each growth had many small brownish pink thin plates that looked shiny in appearance. The pieces took no specific shapes. They ranged in sizes but were around 3mm by 3mm wide and less than 1 mm thick. They were brittle and generally had uniform thickness. If the crystals are consistant with literature, the surface of the plates should correspond to the ab plane of the crystal structure[5]. Other pieces were black in colour. The black pieces occurred more in the cold zone of the ampule.

For the 0.2 growth, EDS was performed. EDS was measured on two different crystals from the growth. For each crystal, various spots were picked to perform EDS. The results can be seen in table 4.1. On different crystals, and at different spots, the expected elements were detected. However, the amounts of each element varied slightly from measurement to measurement. This variation could be due to inhomogeneity. However, the variation could also have been generated from the fact that EDS is not accurate enough to give quantitative results. It is useful for qualitative results. Therefore, it can not be determined if the crystals are homogeneous or not. The data can only show that the crystals have the correct elements.

Using the data from table 4.1 an average can be taken to qualitatively examine the composition. This is done by averaging the results from table 4.1, then rescaling the values with Ti set to 1, and then repeating the rescaling with Se set to 2. These rescaling factors are chosen because we expect the Ti and Se to be in a 1:2 ratio. By taking these two sets of rescaled values, an average can be taken to give the best rescaled values for analysis. Table 4.2 shows the results from this process.

After this rescaling, the amounts of Ti, Se, and Cu were indeed qualitatively in the range that was expected. Thus, it can be argued that the crystals are of the right chemical composition because the Cu concentration was an acceptable amount

Table 4.1: EDS for Cu_xTiSe_2 from the 0.2 growth

Normalized Atomic Percent	Ti	Se	Cu
Crystal 1 - Position 1	32.64	64.62	2.74
Crystal 1 - Position 2	33.05	64.48	2.47
Crystal 1 - Position 3	33.25	64.05	2.70
Crystal 1 - Position 4	31.35	66.01	2.63
Crystal 2 - Position 1	33.37	63.73	2.90
Crystal 2 - Position 2	36.16	61.17	2.66

Table 4.2: Analysis of the EDS results for Cu_xTiSe_2 from the 0.2 growth

Element	Ti	Std. dev.	Se	Std. dev.	Cu	Std. dev.
Average	33.303	1.580	64.010	1.596	2.683	0.141
Fixed Ti=1	1	0.047	1.922	0.048	0.081	0.004
Fixed Se=2	1.041	0.049	2	0.050	0.084	0.004
Average of Fixes	1.0205	0.048	1.961	0.049	0.083	0.004

being between 0 and the intercalation limit of 0.11. The percent of Cu can be argued to be roughly around this value of 8 percent from these results. It is not possible to determine if there is a lack of Se in the crystals because it requires a more accurate measurement.

Susceptibility measurements were employed to determine if any of the crystals were superconducting above 1.8 K. One typical result of the measurements is in figure 4.1. In this figure the magnetic moment is shown. This is proportional to the susceptibility. The crystal measured in figure 4.1 had a mass of 0.29 mg and was placed in a magnetic field of 10 Oe. The crystal was zero field cooled and measured from lower to higher temperatures. The data in figure 4.1 shows that the susceptibility goes from a negative number at low temperature and as temperature is increased the susceptibility increases and approaches zero.

In order to interpret this result, the susceptibility of superconductors needs to be discussed in brief. Susceptibility measurements of superconductors should have a value of -1, which arises from the perfect diamagnetism. As temperature is varied, this value shall stay the same until the critical temperature is reached. Above the critical temperature, the material is no longer a superconductor. Since these non superconducting states are usually metallic, paramagnetic effects should arise.

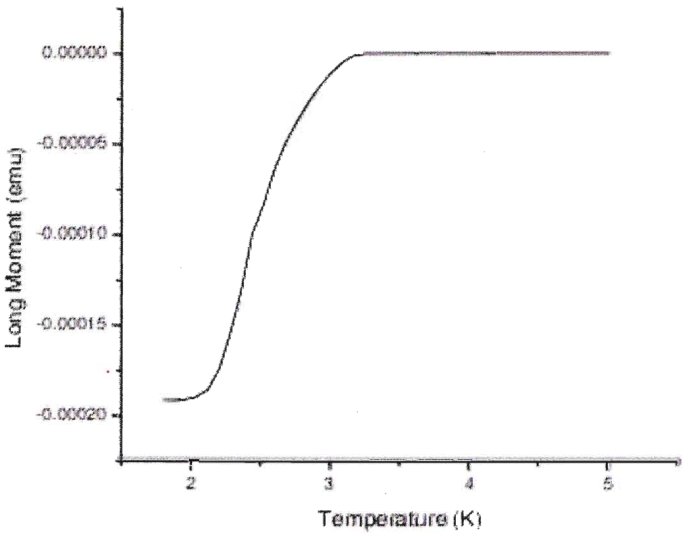

Figure 4.1: Susceptibility measurement from a single crystal from the hot zone from the 0.2 ratio growth.

Since the paramagnetism is orders of magnitude smaller than the diamagnetism in this case, the results should resemble a step function starting at a large negative susceptibility and stepping up to a small positive value.

The result in figure 4.1 shows a transition for 1.2 K rather than a step function. The reasoning for this is easily explained by an arguement that the measured crystal has an inhomogeneous Cu concentration. If the Cu concentration is inhomogeneous, different parts of the crystal would superconduct at different temperatures. There would be many transition temperatures in this case. Thus, if the susceptibility is measured with respect to temperature, there will be a broadening of the transition. Hence, the broadening observed in figure 4.1 is a clear indication that the Cu concentration is not homogenous within the crystal itself.

From figure 4.1, the superconducting state has an onset around 3.3 K. The material seems to be almost fully superconducting around 2.1 K. For other single crystals that were measured, the SC onsets varied. Figure 4.1 was the highest onset from the 0.2 growth. The highest onsets found from the 0.3 growth was 2.4 K. All single crystals measured in the 0.3 growth that were superconducting, did not show signs of complete superconductivity at 1.8 K. In the 0.4 growth, no superconducting state was noticed as the system reached 1.8 K. In all growths, no superconductivity was observed when measuring the black material or any materials from the cold zone. All superconductors were pinkish brown in colour, but not all of the crystals

of this colour were superconducting.

By comparing the onsets of superconductivity from the 0.3 growth and the 0.4 growth it seems that both growths had too much Cu since with more Cu in the reactants the superconducting transition was decreasing. Since the reactants in the 0.2 growth may not have been the correct ratio, it is necessary to grow crystals around this ratio to form more conclusions.

4.2 Growths to Re-examine the 0.2 $CuCl_2$:$TiSe_2$ Ratio

Two growths were attempted with ratios of 0.17 and 0.23 of $CuCl_2$ to $TiSe_2$. At the end of each growth, product could be seen in the cold and hot zone of the ampule, just like in the previous growths. Once again, each growth had many small brownish pink thin plates that looked shiny in appearance as well black pieces. The pieces had the same visual characteristics as reported for the previous growths.

There was enough single crystals of the 0.23 growth so that x-ray diffraction could be measured. The diffraction pattern with labelled Miller indices can be seen in figure 4.2. The peaks that were not labelled with Miller indices were caused by diffraction from the mount that was used. The positions of the peaks were plugged into DICVOL and the output can be seen in Appendix C. The a and c lattice parameters were determined to be 3.540 $\mathring{A}$ and 6.025 $\mathring{A}$ with standard deviations of 0.003 $\mathring{A}$ and 0.004 $\mathring{A}$, respectively.

By comparing the a and c lattice parameters to figure 1.3, it is clear that the numbers are in qualitative agreement. The standard deviation of the parameters are rather large in comparison to the errors reported in figure 1.3. Due to the large standard deviations, a comparison can not be made using the a and c lattice parameters in order to determine a Cu concentration. For brevity, if the standard deviation is neglected and then the comparison is made, it seems in this case, the Cu concentration is on the low scale of optimizing the superconducting transition temperature. Also it can be noted that the a and c lattice parameters do not agree with each other with respect to Cu concentration. Figure 1.3 was a measurement performed on a poly crystalline pellet, where the a and c lattice parameters calculated here were based off of the combination of many single crystals being ground down into a powder. The difference could be due to one measurement being done on a poly crystalline pellet, where the other is done on many single crystals at once. As for the a and c lattice parameters from this measurement indicating that there is a lack of copper is deceiving. In previous growths it was determined that the single crystals have various Cu concentrations. Thus, this measurement is representing more of an average, and this is why the standard deviation is so large. Therefore

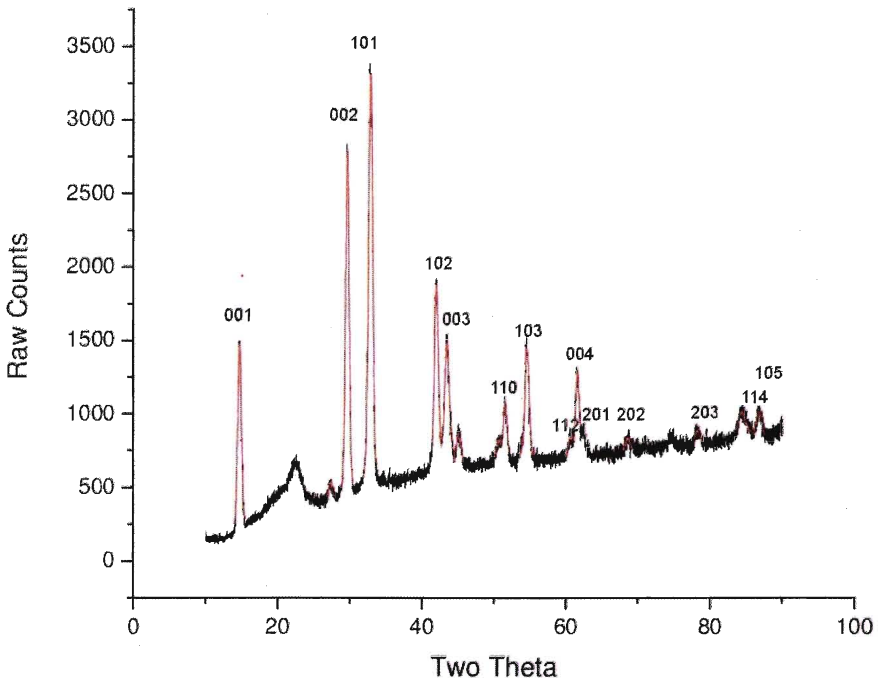

Figure 4.2: The x-ray diffraction pattern measured on Cu_xTiSe_2 from the 0.23 $CuCl_2$:$TiSe_2$ growth ratio. The red curves are the gaussian fits.

certain crystals may indeed have higher amounts of Cu concentration than seen in this comparison.

Susceptibility measurements were employed on single crystals from these two growths to determine if any of the crystals were superconducting above 1.8 K. Superconductivity was found in both sets. The maximum onsets were 2.8 K and 2.5 K respectively. Superconductivity was not complete in any measurements when the temperature reached 1.8 K. The results from measuring the susceptibility of the crystals from the cold zone as well as the black crystals gave results typical to the results found in the previous growths; there was no SC state found. The superconductors that were found, were from the hot zone and were pinkish brown in colour, but not all pinkish brown crystals were superconducting.

By comparing the superconducting onset temperatures from the 0.17 and 0.23 growth it seems like the optimal onset has not been found and there is room for improvement. By looking at the electronic state diagram in figure 1.8 and realizing that the onset temperature is decreasing as the reactant ratio is increasing, reducing the growth ratio may improve the superconducting onset. The only exception would be if the optimum ratio exists between 0.17 and 0.23. Therefore, growths of a reactant ratio below 0.17 may give the optimum superconductivity. Since growths attempted before in the range of a ratio of 0.10 did not produce superconductors, a more methodical approach should be taken. The growth should be more systematic in nature because there may be other factors besides the reactant ratio that effects the superconducting onset.

4.3 Systematic Growths Below the Ratio of 0.17 $CuCl_2$:$TiSe_2$

Four growths were attempted with 0.08, 0.10, 0.12, and 0.14 ratios of $CuCl_2$ to $TiSe_2$. These growths were more systematic in nature. One of the changes that made the growths more systematic in nature was that the $TiSe_2$ was grown first and then divided equally into four so that each growth had the same starting material. A side effect to this process is now the growths had only one forth of the $TiSe_2$ they previously had. This was unavoidable because only so much $TiSe_2$ could be made in one process because too much material in the same sized ampule would lead to too much pressure on the quartz ampule during the heating process. Too much pressure in the heating process would make the quartz ampule explode. Another change was that the ampules were all placed in a larger oven. This was done so they can be placed side by side to experience exactly the same heating process. The point of these changes were to minimize the difference between the growths to create results that would be easier to draw conclusions from.

At the end of these growths, product was only seen in the hot zone. This was the

first difference noticed between these growths and the previous growths. Logically, this could be from the reduction of reactants because this is the only change that can effect this. This agreement seems to be reasonable because there may not be enough material for product to form in the cold zone. It was also noted that each growth had many small brownish pink thin plates that looked shiny in appearance. This was consistent with the previous growths. However, in these growths there was no black pieces to be found. The explanation for lack of black pieces in the product is the same arguement as to why no product was found in the cold zone.

Susceptibility measurements were employed again to determine if any of the crystals were superconducting above 1.8 K. Superconductivity was found in all the growths. Just like in previous growths, the SC onsets, in each growth, varied from crystal to crystal and not all of the pinkish brown crystals were superconducting above 1.8 K. The maximum SC onsets found in each growth were 3.1 K, 3.9 K, 3.0 K, and 2.8 K respectively. Most of the crystals measured were not fully superconducting when the temperature reached 1.8 K. Thus, the Cu concentration was not homogenous in these crystals either.

For convenience all the maximum superconducting onsets have been plotted with respect to the reactant ratio in figure 4.3. Clearly, the 0.10 growth ratio gives the

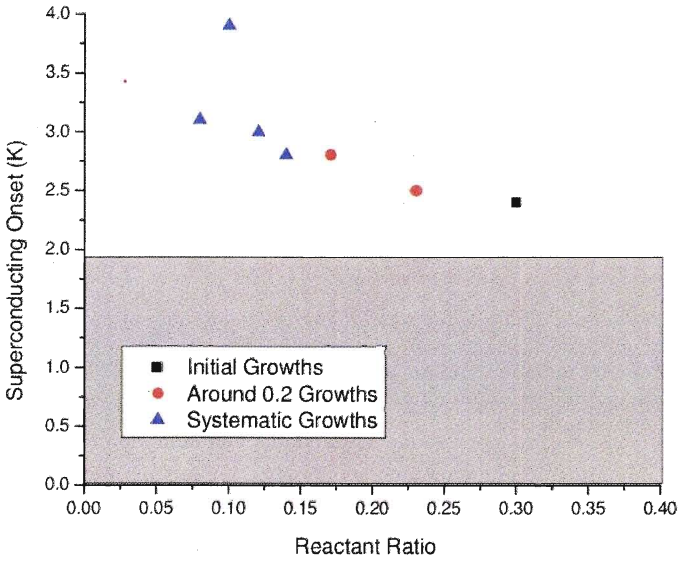

Figure 4.3: The maximum superconducting onset found in each growth

best superconducting onset. This growth ratio could be creating some crystals with

a Cu concentration close to 0.08.

The susceptibility was measured at higher temperatures also to see if there were patterns that related to the amount of Cu as was discussed in the Introduction for poly crystals. One of the high temperature susceptibility measures can be seen in figure 4.4.

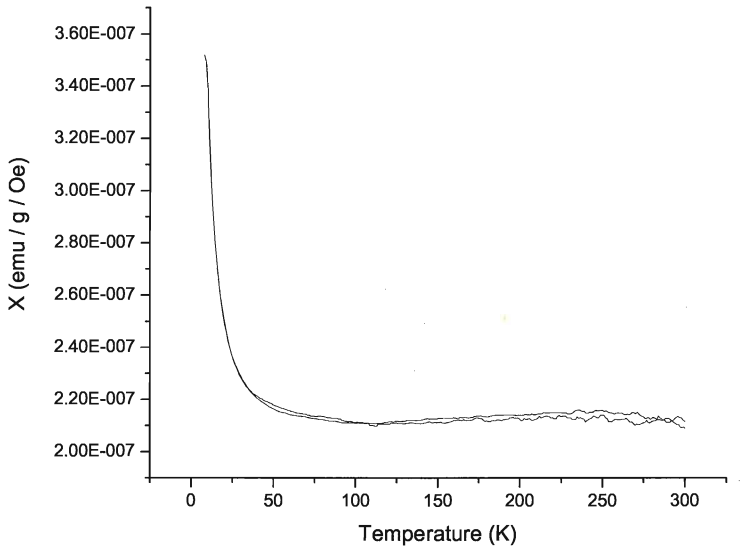

Figure 4.4: Susceptibility measurement from a group of single crystals from the 0.08 ratio growth.

The curve in figure 4.4 is the same as a typical paramagnetic curve when there is a temperature dependence on the paramagnetism. The data was taken from 5 K to 300 K then back down to 5 K allowing to see the zero field cooled and field cooled measurements on the same graph. The two measurements should coincide. The small difference between the two curves measured is due to noise in the measurements.

In the higher temperature susceptibility measurements, no clear relations could be determined between the reactant ratio and the susceptibility measured on crystals at 300 K. It is reasonable not to find a pattern because the Cu concentration per crystal varies within the growth. Therefore, there is no clear pattern expected between susceptibility and crystal growth reactant ratio. The only way to verify this relation would be to know the Cu concentration for each single crystal measured.

Resistivity measurements were taken on various crystals from various growths. All resistivity measurements were setup to measure the resistivity through the ab

plane. Measuring the resistivity has two advantages: The first advantage is it allows for a more indepth analysis on how the material superconducts when it is compared to susceptibility measurements. The second advantage is it may be used to determine the Cu concentration. This is done by examining the residual resistivity ratio (RRR) for various crystals because in literature a relationship has been found where the Cu concentration varies with this ratio[2]. RRR in this circumstance is a ratio of the resistivity at 300K/5K. The RRR for single crystals have been reported to be approximately a value of 2 when there is no or very little amounts of Cu. The RRR increases and maximizes around 5 as the amount of Cu is increased in the crystals.

Figure 4.5 is a resistivity measurement taken for one single crystal and the superconducting transition for this crystal is shown again in figure 4.6. Another

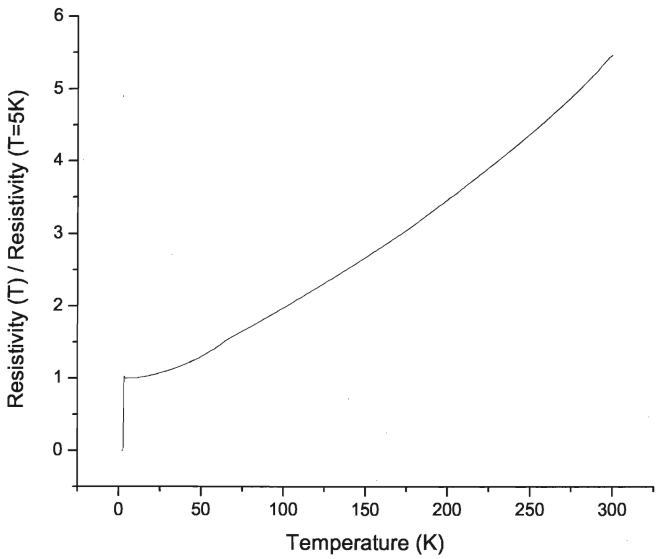

Figure 4.5: Normalized resistivity measurement on a single crystal from the 0.10 $CuCl_2$:$TiSe_2$ growth.

resistivity measurement on another crystal from the same growth focused on the superconducting transition can be seen in figure 4.7.

Figure 4.5, from 5 K to 300 K, had the same curve as reported from other resistivity measurements. It can be read that the RRR is approximately 5.5. This value is in the expected range for Cu_xTiSe_2 but shows that the Cu may be close to the intercalation limit. The RRR's, in a single growth, varied from crystal to crystal However, all values were between approximately 2 and 5.5 for all growths. This range of RRRs were expected. These results also indicate that Cu concentration in each

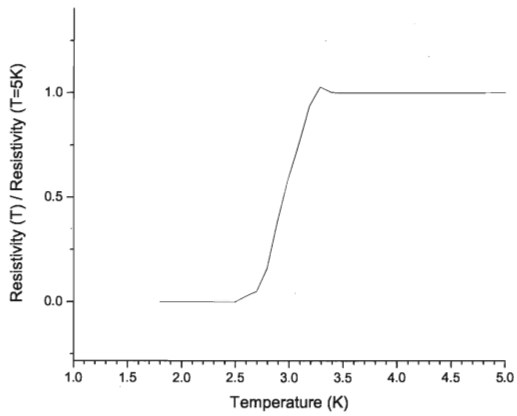

Figure 4.6: The superconducting transition from figure 4.5

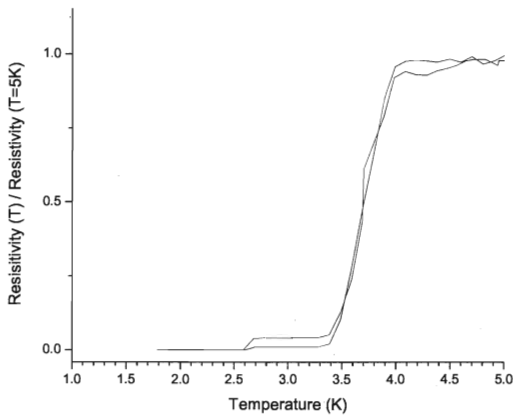

Figure 4.7: The superconducting transition from a single crystal in the 0.10 $CuCl_2$:$TiSe_2$ growth

growth is varying crystal to crystal.

The onset seen in figure 4.6 occurs at 3.3 K and it shows signs of complete superconductivity at 2.6 K. Figure 4.7 shows similar characteristics but the onset is 3.9 K and the transition completes at 3.4 K. Figure 4.7 shows that this growth has produced crystals with a SC onset very close to the optimum. From the 0.08 growth and the 0.10 growth the highest onsets were found to be at 1.8 K and 3.9 K respectively. There were no superconducting transition noticed in all the resistivity measurements on crystals from the 0.12 and 0.14 growths.

By comparing the resistivity in figure 4.6 and figure 4.7 to magnetic susceptibility data, as seen in figure 4.1, it is noticed that the broadness of the SC transition is wider in the magnetic susceptibility data. This difference can be explained and give insight into how the sample is superconducting. If there is a sample that has an inhomogeneous SC transition, the susceptibility measurements will show this, as discussed previously. Resistivity measurements do not have this ability. The broadness of the transition in the resistivity data is dependant on which parts of the crystals are superconducting. Once there is a complete SC pathway built from the SC parts connecting the contacts made for resistivity measurements, the resistivity will go to zero. Thus, in the resistivity measurement, the material will look completely superconducting at this point. The broadening in the resistivity measurements occur when there are SC areas but they are not completing a pathway connecting the contacts. This is why the broadening in the resistivity measurements can be shorter than the broadening in the susceptibility measurements. Other resistivity measurements were typical to figure 4.6 and figure 4.7.

Out of all of the systematic growths, one growth was able to produce very close to the highest superconducting temperature seen. Each growth itself has inconsistencies of Cu concentration from crystal to crystal. Additionally, each crystal itself has an inhomogeneous Cu concentration. The crystals with the highest superconducting temperatures found may be useful for PCS, and will be measured. The only improvement that can be made would be to minimize the inhomogeneity. Poly crystaline growths were attempted since there was a annealing step which could reduce the inhomogeneity.

4.4 Polycrystaline Growths and Characterization

Polycrystaline growths were attempted to see if there would be more homogeneity in the pellets as well as the growths. Four growths were attempted, where in each growth, the amounts of the starting material of Cu was varied. $TiSe_2$ was left over from single crystal growths, so this was also used to create undoped $TiSe_2$ for comparison reasons. At the end of each growth, purple-grey pellets were

found. Purple-grey pellets were also found by Morosan et al. for their polycrystalline growths[3].

X-ray diffraction was performed on various pellets from various growths. A typical diffraction pattern with labelled Miller indices can be seen in figure 4.8. All

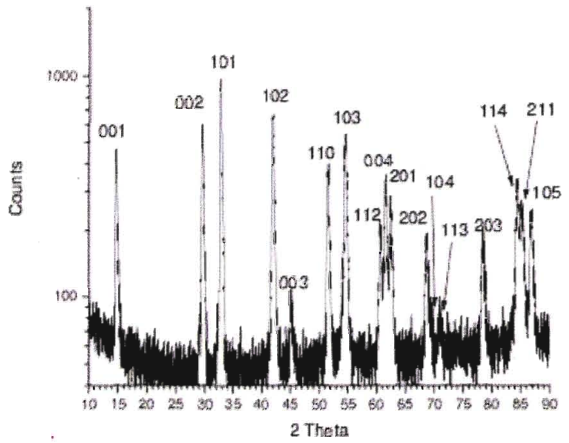

Figure 4.8: An x-ray from one of the polycrystalline growths

other data from x-ray diffraction were very close in appearance to figure 4.8. The difference between the sets of x-ray data was that the peaks were slightly offset from one set to another. This was expected because Cu expands the a and c lattice parameters. Thus different Cu amounts would cause this. DICVOL, which is a program to analyze x-ray diffraction data, was used to help analyze the results. By providing the locations of the peaks on the x-ray diffraction data, the a and c lattice parameters for each growth as well as the standard deviation was extracted. The a and c lattice parameters and the standard deviations can be seen in table 4.3. An example of the output to determine the a and c lattice parameter can be seen in Appendix C. For a more indepth explanation of the analysis, refer to the Experimental Techniques chapter.

The a and c lattice parameters are in the range of what was expected for the growths since the values are comparable to other reported a and c lattice parameters as seen by comparing the results to figure 1.3. The values have a fairly large standard deviation in comparison to figure 1.3. Therefore, the Cu concentration of each pellet can not be determined by comparing the two pieces of data.

Susceptibility measurements were employed to determine if any of the pellets were superconducting above 1.8 K. Superconductivity was found in a few of the growths. The superconducting transition temperatures varied from growth to growth

Table 4.3: a and c lattice parameters found from various pellets. Growth 0 denotes the non doped pellets and the * is the pellet where the onset may exist.

(Growth)-(Pellet)	0-1	1-1	2-1	3-1	4-1	4-2	4-3
a Parameter ($\AA$)	3.5405	3.54067	3.53953	3.53806	3.54536	3.54029	3.54065
Std. Dev. of A ($\AA$)	0.00028	0.00108	0.00096	0.001	0.00453	0.00066	0.00152
c Parameter ($\AA$)	5.99078	6.02187	6.01861	6.02652	6.00703	6.0213	6.02221
Std. Dev. of C ($\AA$)	0.00047	0.00179	0.00195	0.00251	0.00588	0.00155	0.00279
onset of SC (K)	None	2.8	None	1.8*	2.0	2.2	3.0

as well as pellet to pellet. The maximum onsets found in two of the growths were at 3.0 K and 2.8 K. In another one of the growths there was a possibility that there was an onset at 1.8 K for one pellet, but the rest of the pellets from this growth had no signs of a SC state. The undoped and the last growth did not show any signs of superconductivity. Superconductivity was not complete in any pellets when the temperature reached 1.8 K. Thus, the Cu concentration was not uniform in these growths also.

The superconducting onset temperature has been added to table 4.3 for convenience. No relationship can be seen between superconductivity and either the a or c lattice parameters. This is due to inhomogeneity, which could be why the a and c lattice parameters calculated have a large of a standard deviation also.

Chapter 5

Point Contact Spectroscopy

5.1 Point Contact Spectroscopy on the 0.2 Growth

PCS was attempted on the single crystals from the 0.2 growth. Numerous measurements of the IV characteristics at 1.8 K were completed by attempting to make a point contact that allowed the electrons to be in a ballistic regime. The current with respect to the electrical potential from two separate crystals can be seen in figure 5.1 and figure 5.2. The IV characteristics seem to have a linear

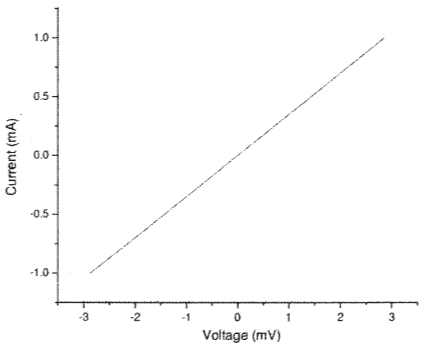

Figure 5.1: IV characteristics using a point contact on a single crystal from the 0.2 growth at 1.8 K

relation. To verify this, the derivative of the data was taken. The results from these can be seen in figure 5.3 and figure 5.4, respectively.

The brief non-linear characteristics in the data are clearly due to noise in the IV data. It is evident that figure 5.3 and figure 5.4 are not comparable to BTK theory. There are a couple of possibilities of why non-linear IV characteristics are not seen that are comparable to BTK theory. If the superconducting transition temperature for the crystals used in the PCS attempts are below 1.8 K, the crystals will not be superconducting and the IV characteristics would be linear in this scenario. Another reason why linear IV characteristics are seen could be due to the point contact being

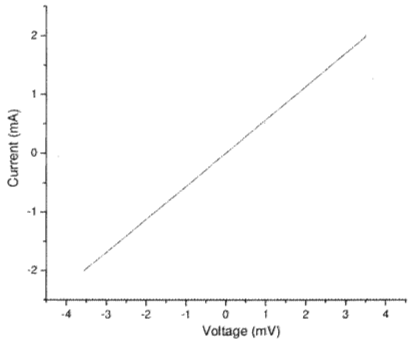

Figure 5.2: IV characteristics using a point contact on another single crystal from the 0.2 growth at 1.8 K

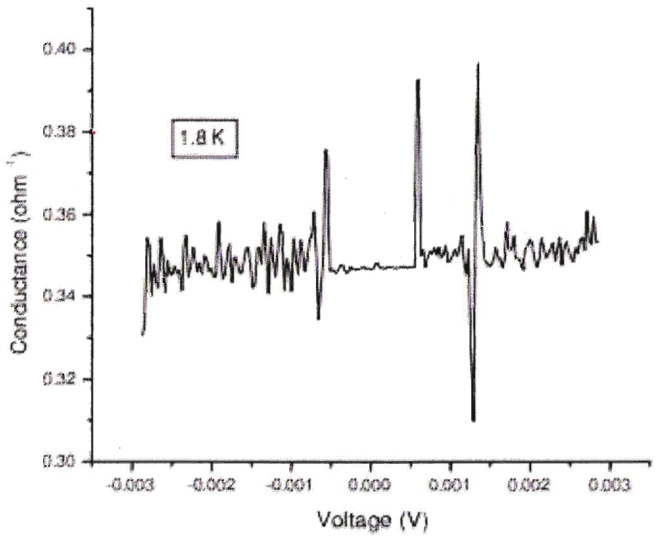

Figure 5.3: Conductivity characteristics using a point contact on a single crystal from the 0.2 growth at 1.8 K

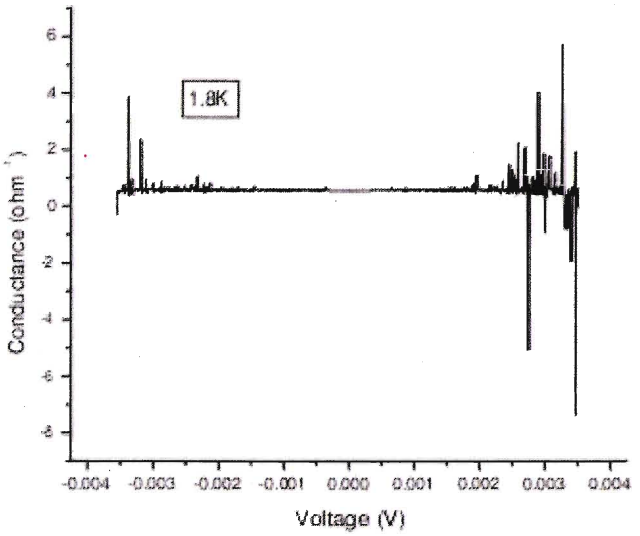

Figure 5.4: Conductivity characteristics using a point contact on another single crystal from the 0.2 growth at 1.8 K

too large. This could create Joule heating, which would raise the temperature at the contact quite significantly bringing the sample well out of the superconducting state. All other IV measurements were typical to these ones presented.

It was noted for this crystal growth that the onsets did vary crystal to crystal, so unless a crystal with a high transition temperature was selected, and concurrently a good point contact was made, desired results would not occur. It is quite possible that both of these factors working together are attributing to the results seen thus far.

According to BCS theory, if a material is superconducting and the temperature is close to the transition temperature, Δ is small[18]. Therefore, even if the transition temperature of some materials is slightly larger than 1.8 K and a good contact is made, it still may be difficult to detect non-linear IV characteristics. This assumption is reached by reasoning that, if there is a small Δ then results in this scenario would only produce slight deviations from the linear IV characteristics. In this case the non-linear characteristics could be mistaken for noise or hidden in noise.

In order to get non-linear IV characteristics, either a system has to be used where it can go down to lower temperature, or single crystals with higher superconducting transition temperatures must be measured. By having a combination of both, it would be more likely to have success. To compare to BCS theory, it requires Δ to be measured for various temperatures. Therefore, not only a result needs to be seen

at the lowest temperature possible, but non-linear characteristics needs to be seen for various temperatures before the superconductivity stops. Thus, improvements are doubly important.

5.2 Point Contact Spectroscopy on the 0.1 Growth

Single crystals from the 0.10 growth were selected for PCS measurements since they had the highest superconducting onsets. Two of the IV characteristics measured at 1.8 K are shown in figure 5.5 and figure 5.6, respectively. Figure 5.5 is

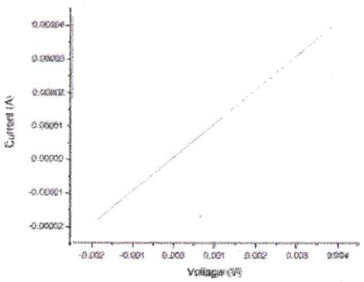

Figure 5.5: IV characteristics using a point contact on a single crystal from the 0.1 growth at 1.8 K

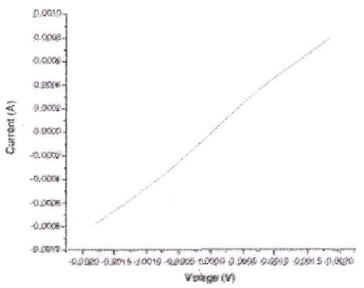

Figure 5.6: IV characteristics using a point contact on another single crystal from the 0.1 growth at 1.8 K

typical to the previous attempts, however figure 5.6 does have non-linear IV characteristics. The derivatives of figure 5.5 and figure 5.6 are seen in figure 5.7 and figure 5.8, respectively.

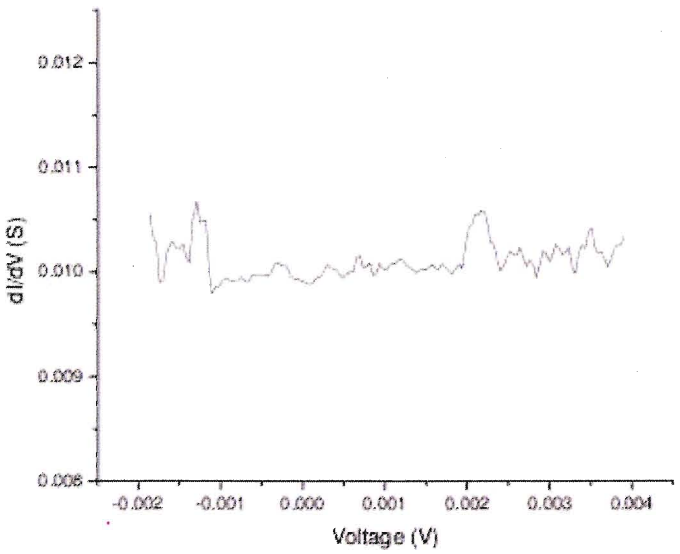

Figure 5.7: Conductivity characteristics using a point contact on a single crystal from the 0.1 growth at 1.8 K

By comparing figure 5.8 to other experimental PCS results, such as Zn, as seen in figure 5.9, it is noted that the conductivity curve looks comparable to one of the curves at higher temperature[34]. Since the IV as well as the conductivity curves are symmetric with respect to the electrical potential, figure 5.8 shows only one peak. This demonstrates that this material is a single gapped superconductor. This was expected, as was discussed in the Introduction. Data at lower temperatures would be able to demonstrate the single superconducting gap more clearly.

The result shown in figure 5.8 does indeed reinforce that, before, the problem was from the superconducting transition temperature of the samples were too low to get PCS results. Also, a system that goes to lower temperatures is necessary. This is necessary because the peaks in the conductivity curves would become visually recognizable, and there would be a possibility to compare data to BCS theory to check for conventional superconductivity.

Fortunately, while these PCS experiments were being measured at Brock University, Dr. Razavi had taken some single crystals from the same growth to the Max Planck institute in Germany to attempt the same experiment. The advantage to measurements being done there was that there were systems that were readily available to go down to temperatures as low as 0.4 K. During his work, many IV characteristics were recorded. Upon inspection of the data, non-linear IV characteristics

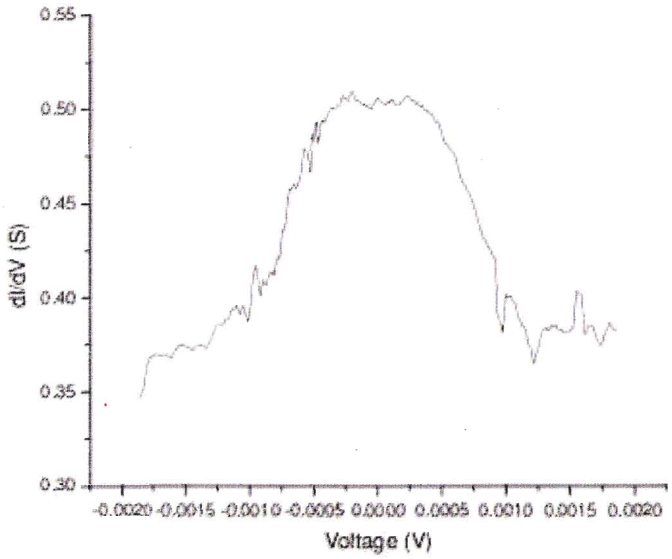

Figure 5.8: Conductivity characteristics using a point contact on another single crystal from the 0.1 growth at 1.8 K

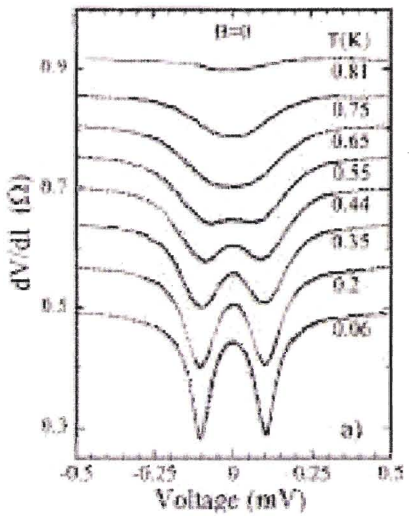

Figure 5.9: Point Contact Spectroscopy measured on Zn[34]

were noted and the normalized conductivity curves results at various temperatures are plotted in figure 5.10.

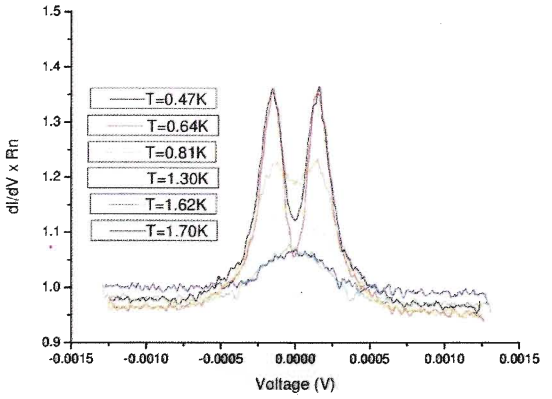

Figure 5.10: A set of PCS measurements taken in Germany by Dr. Razavi on a single crystal from the 0.2 growth

In figure 5.10, it can be argued again that the superconductor has only a single gap since the second peak is due to symmetry. By looking at figure 5.8 and comparing it to figure 5.10, figure 5.8 measured at 1.8 K looks most like the measurement in figure 5.10 at 1.7 K. Therefore, the results on two independent systems seem to be consistant. To analyze these results further, fitting the functions to theory to extract the physical parameters is essential.

5.2.1 Creation and Verification of Fitting Programs

In order to fit the experimental data to theory, a fitting program must be written to do so. The first step would be to replicate the theoretical functions. Equation 2.13 was the first function to be replicated. The integral is not known to have an analytical solution, so the integration must be numerically solved. An algorithm that utilized Riemman sums were used to complete this task. To handle the infinite limits of integration, smart choices were made to only integrate in a finite range because the integrand is significant only for a certain range of values. After building the program to do this, IV curves for various Z values and temperature were generated. For zero temperature, IV curves were generated in order to compare to BCS theory.

Figure 5.11 are a compilation of some outputs with zero temperature. These sets of data were chosen to compare to figure 2.5. The two figures are in agreement

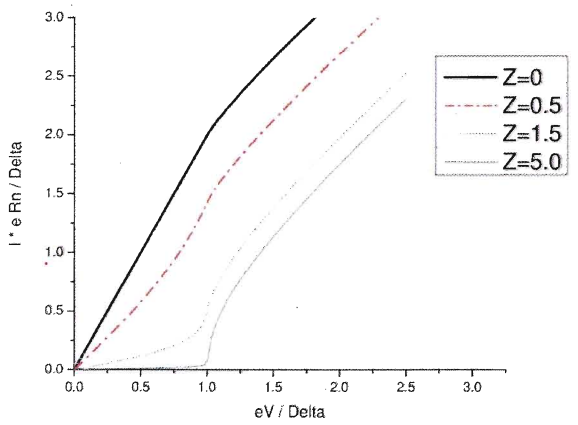

Figure 5.11: Replication of the IV curves from BTK theory

with each other. The derivative of the data in figure 5.11 was taken and can be seen in figure 5.12. This figure can also be compared with figure 2.6. Both of these figures are also in agreement with each other. Therefore, equation 2.13 was solved properly, and now can be used for fits to experimental data.

There was a modification to BTK theory that Plecenik et al. suggested, as discussed in the Theoretical Background chapter[24]. A program was built to replicate this modified BTK theory. The changes were applied to the program that could replicate BTK theory. Figure 5.13 are some conductivity curves at zero temperature and with Z being 0.5 for various Γ's. The modification reduces and smears the peaks in the conductivity curves. This was expected for this modification. Therefore, this program is working as expected. A small modification to this program can be done to make changes that Mitrovic and Rozema suggest[25].

Since all the theoretical equations were replicated, the next step would be to create a program that finds the best fit between the experimental data and the theoretical equations. The program's code was written to utilize the Levenberg-Marquardt method. A more detailed discussion of this method can be found in the Experimental Techniques chapter. The Levenberg-Marquardt method requires a solution of a system of linear equations. Therefore an algorithm was written to do Gauss-Jordan elimination in order to solve the system of linear equations. The method also requires derivatives with respect to the fitting parameters. Due to the difficulty, as well as length of time it would take to create analytical derivatives, if it was possible, numerical derivatives were taken instead. This was done and the fitting program utilizing the modified BTK theory can be found in Appendix A. This program was tested on data that was available for $Cd_2Re_2O_7$ that Dr. Razavi

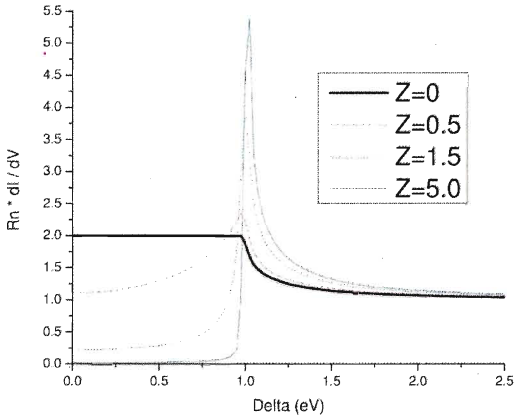

Figure 5.12: Replication of the conductivity curves from BTK theory

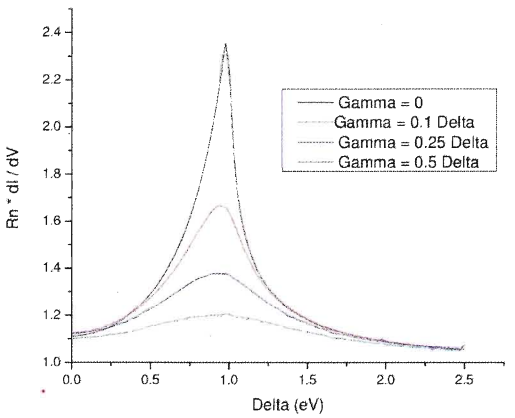

Figure 5.13: Generation of conductivity curves from a modified BTK theory

has measured the IV characteristics on previously. The results of the fits can be seen in figure 5.14.

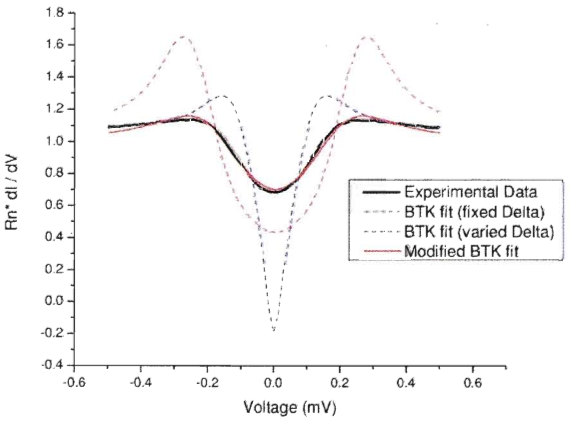

Figure 5.14: Various fits to experimental $Cd_2Re_2O_7$ PCS data

Various fits were chosen. The analysis of the fits and the reason why some of the fits were not good fits are explained later. The importance of figure 5.14 is that it shows the fitting program is in good working condition and is ready to be used for Cu_xTiSe_2 data.

The temperature dependence on the energy gap from BCS theory needed to be replicated also. Equation 2.9 is the equation that is needed. Since this equation has no analytical solution, an algorithm was written to find the numerical solution for Δ when all other parameters are known. The integration was once again dealt with by using Riemann sums and by making a substitution of variables to make the limits of integration finite. One result from this program, where Δ and the temperature were normalized, can be seen in figure 5.15. This is in agreement with figure 2.3. Therefore, the prediction from BCS theory has been replicated, and this function could be used for fits also.

Since this theoretical function was repeated, a fitting program to experimental data could be built. The same techniques and tricks were used to create this program, just like the program for the fits to BTK theory. The code of fitting program can be found in Appendix B.

It is now possible to further analyze experimental PCS data. These programs could be used to extract physical properties and to determine if there are quasiparticle lifetime effects. By trying to fit the data to BCS theory, it can be determined if the material agrees with the theory for conventional superconductivity.

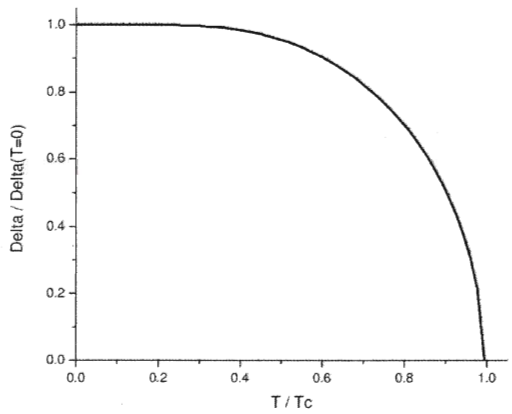

Figure 5.15: Replication of the temperature dependence of the energy gap from BCS theory

5.2.2 Fitting Experimental Data to Theory

In order to determine the best theory to fit the data to, three fits were attempted. The first fit was based on BTK theory but Δ was fixed because it could be determined directly from the conductivity curves. The second fit was based on BTK theory again, but this time Δ was allowed to optimize. The last fit was the modified BTK function presented by Plecenik et al. where a lifetime of quasiparticles was accounted for. All of the fits can be seen in figure 5.16 and parameters that corresponded to the fits are in table 5.1.

Table 5.1: Results from the fits that can be seen in figure 5.16

Fit Type	Δ (meV)	Z	C	Γ (meV)
BTK - fixed Δ	0.15	0.680	1.042	N/A
BTK - varied Δ	0.128	0.650	1.023	N/A
Modified BTK (Plecenik)	0.141	0.600	1.006	0.0194

In figure 5.16, the best fit of the three is when a modification to the BTK theory is used. Therefore, there is a quasiparticle lifetime effect. For the two other fits, the fits had trouble replicating the experimental data. For example, when Δ was allowed to vary for the BTK theory, the peak in the theory did not align with the

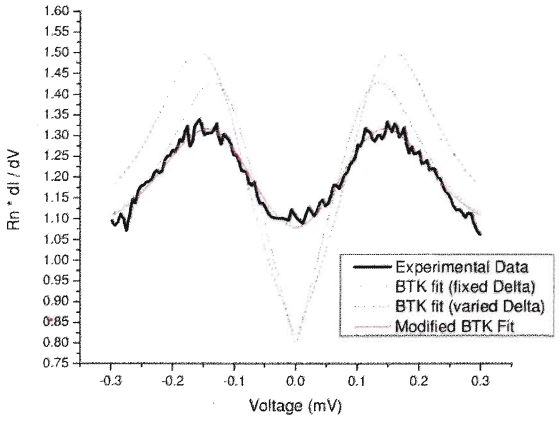

Figure 5.16: Various Fits to Experimental PCS. T=0.42K

experimental peak. Also, there was a large gap between the experimental data and the curve of the fit. It is clear that the quasiparticle lifetime effect has significance in this measurement.

The data was fitted again using the fitting program where there was a modification to the BTK theory but it was changed to take into account the suggestion made by Mitrovic and Rozema, as discussed in Theoretical Background chapter[25]. The fit to the experimental data is plotted in figure 5.17. This modification to the

Table 5.2: Results from the fits that can be seen in figure 5.17

Fit Type	Δ (meV)	Z	C	Γ or iΔ (meV)
Plecenik	0.141	0.600	1.006	0.0194
Mitrovic	0.143	0.582	1.002	0.0203

fit essentially made no difference. The parameter to the fits can be seen in table 5.2. The values are very close to each other when comparing between the two fits. Since the imaginary parts are small compared to the Δ's, the fits from these two were expected to be the same[25].

All other data was theoretically fitted using the modified BTK theory suggested by Plecenik et al[24]. The results are seen in table 5.3. The best fits occurred always when a modification to BTK theory was used. The Γ parameter was small in comparison to Δ, therefore the suggestion by Mitrovic and Rozema was not

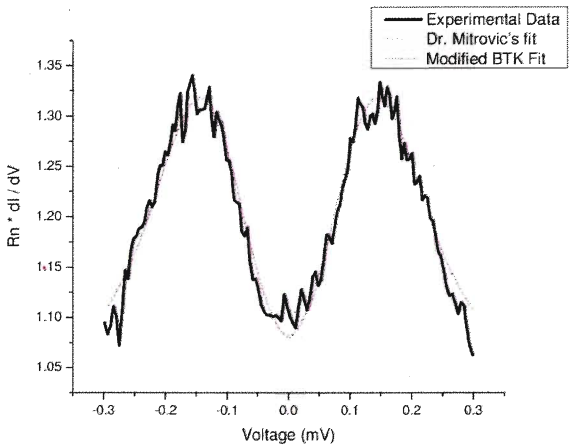

Figure 5.17: Comparison of Modified BTK Fits to Experimental PCS. T=0.42K

needed[25]. The variation in Γ is not understood. The large change in Z at warmer temperatures could be due to the fit not requiring a high degree of accuracy on this parameter on the data at these temperatures. Z may experience thermal effects but they would cause Z to increase as temperature increases. Since Z is related to the barrier potential, this was not expected to vary, and seeing that it is not a large value this means that the scattering at the contact is not large. The C parameter is used to normalize the data, since the data was already normalized, the value should be expected to be 1. As seen in table 5.3, all values are around 1 as was expected.

The Δ's for various temperatures were attempted to be theoretically fit to BCS theory. The fits had physical complications. In order for the Merit function to be optimized, the optimized T_c had to be quite a bit less in temperature than where the Δ's became zero. Therefore, it was more reasonable to force the T_c where Δ became zero. Thus, the T_c was set to 1.75 K. The plot of this can be seen in figure 5.18.

By examining figure 5.18, it is clear that the experimental data does not correspond to the predictions of BCS theory. If the transition temperature was increased beyond 1.75 K, the experimental data and BCS theory would only diverge. The disagreement between theory and experimental result could not be due to the inhomogeneity in the crystal. The crystal has a continuous inhomogeneity, therefore Δ would be continuous also. This would only broaden the peak, but not shift the peak with respect to the electrical potential. This broadening of the peak would occur more when the temperature of the material gets closer to the superconducting transition temperature because this is the region where delta varies the most with respect to temperature. There is a possibility that Cu_xTiSe_2 is not a conventional superconductor. However, as discussed in the Introduction, this material was

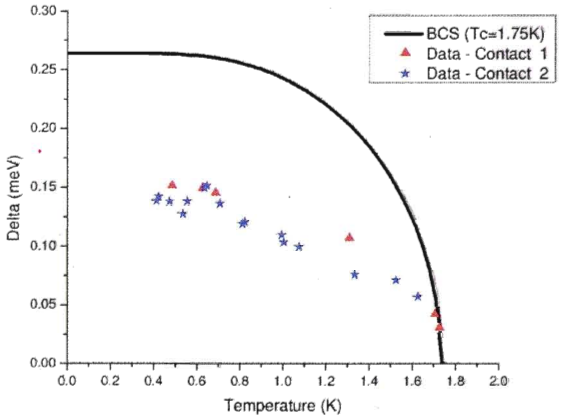

Figure 5.18: Plot of Δ vs.temperature for Cu_xTiSe_2. BCS curve is fixed at T_c=1.75K.

expected to be a conventional superconductor. BTK theory is based off of a 1D model. Cu_xTiSe_2, is an anisotropic material. Therefore, this disagreement could be the cause of BTK theory not taking into account anisotropic effects. Also, the superconducting energy gap could be anisotropic also too. This could also contribute to a disagreement.

5.3 Point Contact Spectroscopy in Temperatures Below 1.8 K at Brock

Another sample from the 0.1 growth was loaded into this new system to measure PCS. The system could not reach any temperatures below 1.8 K. This could have been due to leaks in the new system, which would have contaminated the He-3 gas, which would not allow the system to cool down any further. Due to the unexpected increase in price of He-3, no other experiments could be attempted.

Table 5.3: Results from the fits that can be seen in figure 5.16. The data in the table is divided because below the line was PCS attempted on the same crystal again but a new point contact was made.

Temperature (K)	Δ (meV)	Z	C	Γ (meV)
0.41	0.138	0.599	1.004	0.0156
0.42	0.141	0.600	1.006	0.0194
0.47	0.138	0.609	1.007	0.0074
0.53	0.127	0.665	0.995	0.000001
0.55	0.138	0.632	0.992	0.00001
0.63	0.149	0.603	0.974	0.00008
0.64	0.151	0.600	0.955	0.00008
0.70	0.136	0.607	0.991	0.00003
0.81	0.118	0.635	0.992	0.00008
0.82	0.120	0.619	0.997	0.000002
0.99	0.109	0.609	0.994	0.000008
1.00	0.103	0.612	0.984	0.00004
1.07	0.100	0.604	0.997	0.00002
1.33	0.075	0.351	0.999	0.0169
1.52	0.070	0.269	1.008	0.0320
1.62	0.056	0.228	1.009	0.0394
0.48	0.151	0.574	1.002	0.0090
0.62	0.148	0.600	0.997	0.00001
0.68	0.144	0.591	0.995	0.00003
1.30	0.107	0.523	1.001	0.0095
1.70	0.042	0.235	1.006	0.0155
1.72	0.031	0.291	1.004	0.0055

Chapter 6

Conclusions

Single crystals of Cu_xTiSe_2 of various doping were obtained. The crystals were verified and characterized with the help of EDS, X-ray diffraction, resistivity, and susceptibility measurements. EDS showed the correct elements to be involved with the composition to be qualitatively in the right proportions. X-ray diffraction showed that the material grown had the proper crystal structure. The a and c lattice parameters determined were in good qualitative agreement with what was expected. Susceptibility measurements showed that superconducting states did exist and that all the crystals were inhomogeneous. Also, in each growth, the Cu concentration varied crystal to crystal. Due to inhomogeneity, the susceptibility measurements at room temperature could not be used for further analysis. The RRR was in the expected region for all single crystals. Due to the inhomogeneity of the growths, no pattern could be verified with respect to the reactant ratios. By comparing the resistivity to the susceptibility it was clear that superconducting pathways form through the ab plane before the material is completely superconducting. When the ratio of $CuCl_2$:$TiSe_2$ was 0.1 the superconducting onset was closest to the optimum onset. It was found that not just the reactant ratio, but the amount of reactant being used in the growth also effects the end product as well as the maximum SC onsets obtained.

Poly crystals of Cu_xTiSe_2 of various doping were obtained. The colour of the pellets was what was expected. X-ray diffraction results were found and the structure was indeed what was expected. The analysis of the x-ray data was used to extract the a and c lattice parameters and were found to be in good qualitative agreement. Susceptibility measurements characterized the superconducting onsets. The measurements also indicated that inhomogeneity was also an issue in these growths.

Point contact spectroscopy was attempted on two different crystal growths. The first growth had an attempted 0.2 reactant ratio of $CuCl_2$:$TiSe_2$. The IV characteristics for various electrical potentials were all the same. They all showed no signs of a superconducting energy gap. This was probably due to the PC being too large or the SC transition temperature being too low. As for the 0.1 growth ratio of $CuCl_2$:$TiSe_2$, non-linear IV characteristics were evident. The conductivity curves with respect to electrical potential were indeed what was expected and it was clear that the material has a single energy gap.

Programs were created to fit the experimental data to theory. The data was fitted to BTK theory as well as a modified BTK theory. The fits showed evidence that the modification was needed. Thus, for this material, quasiparticle lifetime effects were evident, which is a product of some form of scattering. The fits to the data were used to determine Δ for various temperatures. The Γ parameters in the fits were small, therefore, there were no complications with the method used to fit the data. When comparing the data to what BCS theory predicts, there is a disagreement. This could be a product of the anisotropy of the material.

Attempts to measure more single crystals at lower temperatures at Brock University were attempted. There were complications, which led to a halt on the experiments.

Bibliography

[1] S. Li, G. Wu, X. Chen, and L. Taillefer. Single-Gap s-Wave Superconductivity near the Charge-Density-Wave Quantum Critical Point in Cu_xTiSe_2. *Physical Review Letters*, 99:107001–1 – 107001–4, 2007.

[2] G. Wu, H. Yang, L. Zhao, X. Luo, T. Wu, G. Wang, and X. Chen. Transport properties of single-crystalline Cu_xTiSe_2 ($0.015 \leq x \leq 0.110$). *Physical Review B*, 76:024513–1 – 024513–5, 2007.

[3] E. Morosan, H. Zandbergen, B. Dennis, J. Bos, Y. Onose, T. Klimczuk, A. Ramirez, N. Ong, and R. Cava. Superconductivity in Cu_xTiSe_2. *Nature Physics*, 2:544–550, 2006.

[4] J. Zhao, H. Ou, G. Wu, B. Xie, Y. Zhang, D. Shen, J. Wei, L. Yang, J. Dong, M. Arita, H. Namatame, M. Taniguchi, X. Chen, and D. Feng. Evolution of the Electronic Structure of 1T-Cu_xTiSe_2. *Physical Review Letters*, 99:146401–1 – 146401–4, 2007.

[5] E. Morosan, L. Li, N. Ong, and R. Cava. Anisotropic properties of the layered superconductor $Cu_{0.07}TiSe_2$. *Physical Review B*, 75:104505–1 – 104505–5, 2007.

[6] H. Barath, M. Kim, J. Karpus, S. Cooper, P. Abbamonte, E. Fradkin, E. Morosan, and R. Cava. Quantum abd Classical Mode Softening Near the Charge-Density-Wave-Superconductor Transition of Cu_xTiSe_2. *Physical Review Letters*, 100:106402–1 – 106402–4, 2008.

[7] M Traum, G. Margaritondo, N. Smith, J. Rowe, and F. Di Salvo. $TiSe_2$: Semiconductor, semimetal, or exitonic insulator. *Physical Review B*, 17:1836–1838, 1978.

[8] K. Woo, F. Brown, W. McMillan, R. Miller, M. Schaffman, and M. Sears. Superlattice formation in titanium diselenide. *Physical Review B*, 14:3242 – 3248, 1976.

[9] R. Bachrach and M. Skibowski. Angle-Resolved Photoemission from $TiSe_2$ Using Synchrotron Radiation. *Physical Review Letters*, 37:40 – 42, 1976.

[10] F. Di Salvo, D. Moncton, and J. Waszczak. Electronic properties and superlattice formation in the semimetal $TiSe_2$. *Physical Review B*, 14:4321–4328, 1976.

[11] Y. Miyahara, H. Bando, and H. Ozaki. Tunnelling spectroscopic study of the CDW energy gap in $TiSe_2$. *Journal Physics: Condensed Matter*, 7:2553–2561, 1995.

[12] T. Kidd, T. Miller, M. Chou, and T. Chiang. Electron-Hole Coupling and the Charge Density Wave Transition in $TiSe_2$. *Physical Review Letters*, 88:226402–1 – 226402–4, 2002.

[13] H. Myron and A. Freeman. Electronic structure and optical properties of layered dichalogenides: TiS_2 and $TiSe_2$. *Physical Review B*, 9:481–486, 1974.

[14] M. Holt, P. Zschack, H. Hong, M. Chou, and T. Chiang. X-Ray Studies of Phonon Softening in $TiSe_2$. *Physical Review Letters*, 86:3799–3802, 2001.

[15] C. Kittel. *Introduction to Solid State Physics.* John Wiley and Sons, Inc, New York, 2005.

[16] R. Thorne. Charge-density-wave conductors. *Physics Today*, pages 42–47, 1996.

[17] G. Gruner. The dynamics of charge-density waves. *Reviews of Modern Physics*, pages 1129–1175, 1988.

[18] J. Bardeen, L. Cooper, and J. Schrieffer. Theory of Superconductivity. *Physical Review*, 108:1175–1204, 1957.

[19] T. Shimojima, Y. Shibata, K. Ishizaka, T. Kiss, A. Chainani, T. Yokoya, T. Togashi, C. Chen X. Wang, S. Watanabe, J. Yamaura, S. Yonezawa, Y. Muraoka, Z. Hiroi, T. Saitoh, and S. Shin. Interplay of Superconductivity and Rattling Phenomena in β-Pyrochlore KOs_2O_6 Studied by Photoemission Spectroscopy. *Physical Review Letters*, 99:117003–1 – 117003–4, 2007.

[20] M. Tinkham. *Introduction to Superconductivity.* McGraw-Hill, Inc., New York, 1996.

[21] M. Crisan. *Theory of Superconductivity.* World Scientific, New Jersey, 1989.

[22] G. Blonder, M. Tinkham, and T. Klapwijk. Transition from metallic to tunneling regimes in superconducting microconstrictions: Excess current, charge imbalance, and supercurrent conversion. *Physical Review B*, 25:4515–4532, 1982.

[23] R. Dynes, V. Narayanamurti, and j. Garno. Direct Measurement of Quasiparticle-Lifetime Broadening in a Strong-Coupled Superconductor. *Physical Review Letters*, 41:1509–1512, 1978.

[24] A. Plecenik, M. Grajcar, S. Benacka, P. Seidel, and A. Pfuch. Finite-quasiparticle-lifetime effects in the differential conductance of $Bi_2Sr_2CaCu_2O_y$/Au junctions. *Physical Review B*, 49:10016–10019, 1994.

[25] B. Mitrovic and L. Rozema. On the correct formula for the lifetime broadened superconducting density of states. *Journal of Physics: Condensed Matter*, 20:015215, 2008.

[26] Y. Naidyuk and I. Yanson. *Point-Contact Spectroscopy.* Springer, New York, 2005.

[27] P. Goodhew, J. Humphreys, and R. Beanland. *Electron Microscopy and Analysis Third Edition.* Taylor and Francis, New York, 2001.

[28] Collaborative Computational Project No. 14. DIVCOL. World Wide Web electronic publication, 2006. http://www.ccp14.ac.uk/ccp/ccp14/ccp14-by-program/dicvol/.

[29] Powder Diffraction File. 00-030-1383. Electronic Database, 2006. International Center for Diffraction Data.

[30] L. van der PAUW. A method of measuring specific resistivity and hall effect of discs of arbitrary shape. *Philips Research Reports*, 13:1–9, 1958.

[31] J. Clarke and A. Braginski (Eds.). *The SQUID Handbook.* Wiley-VCH Verlag GmbH and Co., Weinheim, 2004.

[32] R. Gonnelli, D. Daghero, and G. Ummarino. Direct Evidence for Two-Band Superconductivity in MgB_2 Single Crystals from Directional Point-Contact Spectroscopy in Magnetic Fields. *Phys. Rev. Lett.*, 89:247004–1 – 247004–4, 2002.

[33] W. Press, B. Flannery, S. Teukolsky, and W. Vetterling. *Numerical Recipes in C: The Art in Scientific Computing.* Press Syndicate of the University of Cambridge, New York, 1989.

[34] Y. Naidyuk, H. Lohneysen, and I. Yanson. Temperature and magnetic-field dependance of the superconducting order parameter in Zn studied by point-contact spectroscopy. *Physial Review B*, 54:16077 – 16081, 1996.

Appendix A

Source Code for the Point Contact Spectroscopy Fits

```
'Author: Mike Potalivo
'Program Name: LM4para_Plec
'Purpose:  Loads in experimental data, and determines the best fit by optimizing
'the fitting paramaters by using the Levenberg-Marquardt method.
'The fitting function is described by Plecenik et. al. which is a
'Modified BTK theory.
'Input: voltage and current from a data file
'Outputs:  1 - the voltage and current from the original data and the fit
'2 - the fit parameters and temperature set


Option Explicit 'Forces variables to be defined

Const RIter As Long = 5000 'Number of iterations in Riemman Sum
Const T As Single = 1.72              'Temperature

Dim RStep As Double          'Step size for Riemann Sum (Integration parameter)
Dim Vmax As Double      'Max voltage value used

Const elec As Double = 1.602176462E-19      'Charge of proton
Const Kb As Double = 1.3806503E-23          'Boltzmann Constant

Private Sub cmdCalc_Click()

Const Normalizer As Single = 1# / 3.8       'parameter to normalize incoming data
Const IterMax As Long = 50                    'Maximum iterations allowed before stopping the fitting routine
Const Sconverge As Single = 0.001   'Stopping parameter, convergence when abs(SumOld-SumNew)/SumNew <Sconverge
Const SConStop As Integer = 2                  'Guarentee convergence. amount of times convergence must be reached
Const Trimmer As Double = 0.0003 * elec 'Truncate useless data

Dim i1, i2 As Long      'For loop counters
Dim i3, i4 As Integer     'Counters
Dim L As Double         'Lambda (LM parameter)
Dim A(3) As Double      'Fitting parameters (Delta,Z, Gamma, C)
Dim x(1000) As Double      'X Data
Dim y(1000) As Double      'Y Data
Dim yT0(1000) As Double     'Theoritically generated y points (set 1)
Dim yT(1000) As Double     'Theoritically generated y points (set 2)
Dim Sum(1) As Double    'Sum of Squares (old and new)
Dim N As Integer        'Number of data points - 1
Dim M(3, 4) As Double   'Alpha (alpha and Beta parameters matrix parameters)
Dim Data(1000) As String      'Lines of Data file
Dim accepted As Boolean    'If the new fit is rejected, a short cut can be taken for the next itteration
Dim SaveM(3, 4) As Double 'Parameters to help out the short cut


'*************************************************************************
'*****************************     INITIALIZATION     ********************
'*************************************************************************

cmdCalc.Enabled = False 'Disabling program controll
accepted = True 'Forcing all values to be calculated

'Initial Guessses
A(0) = 0.00004 * elec 'Delta (units of Joules)
A(1) = 0.55 'Z (potential barrier)
A(2) = 0.00001 * elec 'Gamma (units of Joules)
A(3) = 1 'Renormalization (just in case the normalization is not perfect)

'Initial Lambda
L = 0.001

'Load in data
N = 0
Open App.Path & "\CuTiSeb\CuTiSe_1_72.txt" For Input As #1
```

```
Do While EOF(1) = False
    Input #1, Data(N)
    N = N + 1
Loop
Close #1

i1 = 0
i4 = 0
Do
    i2 = InStr(Data(i1), " ")
    i3 = InStr(i2 + 1, Data(i1), " ")
    x(i4) = Abs(Val(Left$(Data(i1), i2)) * elec)
    y(i4) = Normalizer * Abs(Val(Mid$(Data(i1), i2, (i3 - i2))))

    If x(i4) < Trimmer Then
        If Vmax < x(i4) Then
            Vmax = x(i4)
        End If
        'MsgBox (i1 & " : " & x(i4) & "  " & y(i4))
        i4 = i4 + 1
    End If
    i1 = i1 + 1
Loop While i1 < N

N = i4 - 1
i3 = 0

MsgBox (N)

'*************************************************************************
'*********************************      PROCEDURE     **********************
'*************************************************************************

'Define box sizes for integration
RStep = (Vmax + 10 * Kb * T) / RIter

'Calculate sum of squares
Sum(0) = 0
For i1 = 0 To N
    yT0(i1) = genI(x(i1), A(0), A(1), A(2), A(3))
    Sum(0) = Sum(0) + (y(i1) - yT(i1)) ^ 2
Next i1

'Loop until convergence or too many iterations
For i2 = 0 To IterMax - 1

    cmdCalc.Caption = "Iteration: " & i2 + 1
    cmdCalc.Refresh

    'Generate Linear Equations for LM
    If accepted = True Then
        Call GenerateEqns(M, A, N, L, x, y, yT0)

        For i1 = 0 To 3
            For i4 = 0 To 4
                SaveM(i1, i4) = M(i1, i4)
            Next
        Next

    Else

        For i1 = 0 To 3
            For i4 = 0 To 4
                M(i1, i4) = SaveM(i1, i4)
            Next
        Next

        For i1 = 0 To 3
            M(i1, i1) = SaveM(i1, i1) * (1# + L) / (1# + L / 10#)
        Next

    End If

    'Solve Linear Equations to extract amount to change parameters
    Call Gauss(M)

    'Calc new sum of squares
    Sum(1) = 0
    For i1 = 0 To N
        'yT(i1) = genI(x(i1), A(0) + M(0, 3), A(1) + M(1, 3), A(2) + M(2, 3))
        yT(i1) = genI(x(i1), Abs(A(0) + M(0, 4)), A(1) + M(1, 4), A(2) + M(2, 4), A(3) + M(3, 4))
        Sum(1) = Sum(1) + (y(i1) - yT(i1)) ^ 2
    Next
```

```
    'Compare Sums and make choices
    If Sum(1) >= Sum(0) Then
        'New is worse than old increase Lambda and go again
        L = L * 10#
        accepted = False
    Else
        'New is better, save values and decrease Lambda and go again
        L = L / 10#
        accepted = True

        'Accept the new coefficent values
        For i1 = 0 To 3
            A(i1) = A(i1) + M(i1, 4)
        Next

        'Accept the new theoritical y values WRT the new coefficents
        For i1 = 0 To N
            yT0(i1) = yT(i1)
        Next

            lblSum.Caption = "DiffSum: " & Sum(0) - Sum(1)
            lblSum.Refresh

        If (Sum(0) - Sum(1)) / Sum(1) < Sconverge Then
            i3 = i3 + 1
            If i3 = SConStop Then
                MsgBox ("Sum of squares has converged.  Exiting")
                Exit For
            End If
        End If

        Sum(0) = Sum(1)

    End If

    lblL.Caption = "Lambda: " & L
    lblZ.Refresh
    lblSum0.Caption = "Sum: " & Sum(0)
    lblSum0.Refresh

    lblDelta.Caption = "Delta: " & A(0) / elec & " eV"
    lblDelta.Refresh
    lblDeltaChange.Caption = "Change in Delta: " & M(0, 4) / elec & " eV"
    lblDeltaChange.Refresh

    lblZ.Caption = "Z: " & A(1)
    lblZ.Refresh
    lblZChange.Caption = "Change in Z: " & M(1, 4)
    lblZChange.Refresh

    lblG.Caption = "Gamma: " & A(2) / elec & " eV"
    lblG.Refresh
    lblGChange.Caption = "Change in G: " & M(2, 4) / elec & " eV"
    lblGChange.Refresh

    lblC.Caption = "C: " & A(3)
    lblC.Refresh
    lblCChange.Caption = "Change in C: " & M(3, 4)
    lblCChange.Refresh

    Form1.Refresh

    If L > 10000000000# Then
        MsgBox ("There could have been trouble converging")
        Exit For
    End If

Next

If i2 >= IterMax Then
    MsgBox ("Failure to converge.  Too Many iterations!")
End If

'Output coefficents
'MsgBox ("iterations= " & i2 + 1)
'MsgBox (Sum(0) & " : " & Sum(1))
'MsgBox ("lambda= " & L)
MsgBox ("Delta= " & A(0) / elec & " eV")
MsgBox ("Z= " & Abs(A(1)))
MsgBox ("Gamma= " & A(2) / elec & " eV")
MsgBox ("C= " & A(3))
MsgBox ("T= " & T & " K")
```

```
'Output data to file
i1 = 0
i4 = 0
Open App.Path & "\CuTiSeb\01Fit_1_72.txt" For Output As #1
    Do
        i2 = InStr(Data(i1), " ")
        i3 = InStr(i2 + 1, Data(i1), " ")
        x(i4) = Val(Left$(Data(i1), i2)) * elec
        y(i4) = Normalizer * Val(Mid$(Data(i1), i2, (i3 - i2)))

        If Abs(x(i4)) < Trimmer Then

            If x(i4) > 0 Then
                Print #1, x(i4) / elec & " " & y(i4) & " " & yT0(i4)
            Else
                Print #1, x(i4) / elec & " " & y(i4) & " " & -1 * yT0(i4)
            End If
            i4 = i4 + 1
        End If
        i1 = i1 + 1
    Loop While i4 <= N
Close #1

'Save parameters
Open App.Path & "\CuTiSeb\01Report_1_72.txt" For Output As #1
    Print #1, "BTK MODIFIED - Plec"
    Print #1, "Delta: " & Abs(A(0)) / elec & "eV"
    Print #1, "Z:     " & Abs(A(1))
    Print #1, "Gamma: " & Abs(A(2)) / elec & "eV"
    Print #1, "Renormalization coefficent: " & Abs(A(3))
    Print #1, "T= " & T & " K"
Close #1

cmdCalc.Caption = "Calculate"
cmdCalc.Enabled = True

MsgBox ("Finished")
End

End Sub

Sub GenerateEqns(ByRef A() As Double, ByRef C() As Double, ByRef N As Integer, ByRef L As Double, ByRef x() As Double, ByRef_
_y() As Double, ByRef yT() As Double)

Dim i1, i2 As Integer  'Counters

Dim dyda, dydb, dydc, dydd As Double 'Holders of values
Dim h As Double

h = 100#

'Reset M
For i1 = 0 To 3
    For i2 = 0 To 4
        A(i1, i2) = 0
    Next
Next

'Generate Alpha matrix and Beta vector
For i1 = 0 To N

    'dyda = gendIdd(x(i1), C(0), C(1))
    'dydb = gendIdZ(x(i1), C(0), C(1))

    'Numerical derivatives
    dyda = (genI(x(i1), C(0) + C(0) / h, C(1), C(2), C(3)) - genI(x(i1), C(0) - C(0) / h, C(1), C(2), C(3))) / (2 * C(0) / h)
    dydb = (genI(x(i1), C(0), C(1) + C(1) / h, C(2), C(3)) - genI(x(i1), C(0), C(1) - C(1) / h, C(2), C(3))) / (2 * C(1) / h)
    dydc = (genI(x(i1), C(0), C(1), C(2) + C(2) / h, C(3)) - genI(x(i1), C(0), C(1), C(2) - C(2) / h, C(3))) / (2 * C(2) / h)
    dydd = yT(x(i1))

    'dyda = x(i1)
    'dydb = 1

    'Alphas
    A(0, 0) = A(0, 0) + dyda ^ 2
    A(1, 1) = A(1, 1) + dydb ^ 2
    A(2, 2) = A(2, 2) + dydc ^ 2
    A(3, 3) = A(3, 3) + dydd ^ 2


    A(0, 1) = A(0, 1) + dyda * dydb
    A(0, 2) = A(0, 2) + dyda * dydc
```

```
    A(0, 3) = A(0, 3) + dyda * dydd

    A(1, 2) = A(1, 2) + dydb * dydc
    A(1, 3) = A(1, 3) + dydb * dydd

    A(2, 3) = A(2, 3) + dydc * dydd


    'Betas
    A(0, 4) = A(0, 4) + (y(i1) - yT(i1)) * dyda
    A(1, 4) = A(1, 4) + (y(i1) - yT(i1)) * dydb
    A(2, 4) = A(2, 4) + (y(i1) - yT(i1)) * dydc
    A(3, 4) = A(3, 4) + (y(i1) - yT(i1)) * dydd

Next i1

'Mirrored terms
A(1, 0) = A(0, 1)
A(2, 0) = A(0, 2)
A(3, 0) = A(0, 3)

A(2, 1) = A(1, 2)
A(3, 1) = A(1, 3)

A(3, 2) = A(2, 3)


'Diagonal Terms
A(0, 0) = A(0, 0) * (1 + L)
A(1, 1) = A(1, 1) * (1 + L)
A(2, 2) = A(2, 2) * (1 + L)
A(3, 3) = A(3, 3) * (1 + L)

End Sub

Sub Gauss(ByRef Matrix() As Double)

Dim Temp(4) As Double
Dim i1, i2 As Integer
Dim r As Double

'If either x, y, or z column is all zeros then halt
For i1 = 0 To 4
    If Matrix(0, i1) = Matrix(1, i1) And Matrix(1, i1) = Matrix(2, i1) And Matrix(1, i1) = Matrix(3, i1) And Matrix(0, i1) = 0 Then
       MsgBox "Column of zeros. Halting"
       End
    End If
Next

'If x in row1 is zero than swap rows
If Matrix(0, 0) = 0 Then
    'If row 2 is swapable
    If Matrix(1, 0) <> 0 Then
        MsgBox "Row Swap with 2 due to x"
        For i1 = 0 To 4
            Temp(i1) = Matrix(0, i1)
            Matrix(0, i1) = Matrix(1, i1)
            Matrix(1, i1) = Temp(i1)
        Next
    'If row 3 is swapable
    ElseIf Matrix(2, 0) <> 0 Then
        MsgBox "Row Swap with 3 due to x"
        For i1 = 0 To 4
            Temp(i1) = Matrix(0, i1)
            Matrix(0, i1) = Matrix(2, i1)
            Matrix(2, i1) = Temp(i1)
        Next

    Else
        MsgBox "Row Swap with 4 due to x"
        For i1 = 0 To 4
            Temp(i1) = Matrix(0, i1)
            Matrix(0, i1) = Matrix(3, i1)
            Matrix(3, i1) = Temp(i1)
        Next
    End If
End If

'First column reduction
For i1 = 1 To 3
    r = Matrix(i1, 0) / Matrix(0, 0)
    For i2 = 0 To 4
        Matrix(i1, i2) = Matrix(i1, i2) - r * Matrix(0, i2)
```

```
    Next
Next

'If y in row2 is zero than swap rows
If Matrix(1, 1) = 0 Then
    'If row 3 is swapable
    If Matrix(2, 1) <> 0 Then
        MsgBox "Row Swap with 3 due to y"
        For i1 = 0 To 4
            Temp(i1) = Matrix(1, i1)
            Matrix(1, i1) = Matrix(2, i1)
            Matrix(2, i1) = Temp(i1)
        Next
    'If row 4 is swapable
    ElseIf Matrix(3, 1) <> 0 Then
        MsgBox "Row Swap with 3 due to x"
        For i1 = 0 To 4
            Temp(i1) = Matrix(1, i1)
            Matrix(1, i1) = Matrix(3, i1)
            Matrix(3, i1) = Temp(i1)
        Next
    'Halt on error
    Else
        MsgBox "y is infinite"
        End
    End If
End If

'Second column reduction
For i1 = 0 To 3
    If i1 <> 1 Then
        r = Matrix(i1, 1) / Matrix(1, 1)
        For i2 = 0 To 4
            Matrix(i1, i2) = Matrix(i1, i2) - r * Matrix(1, i2)
        Next
    End If
Next

'If z in row3 is zero than swap rows
If Matrix(2, 2) = 0 Then
    'If row 4 is swapable
    If Matrix(3, 2) <> 0 Then
        MsgBox "Row Swap with 4 due to y"
        For i1 = 0 To 4
            Temp(i1) = Matrix(2, i1)
            Matrix(2, i1) = Matrix(3, i1)
            Matrix(3, i1) = Temp(i1)
        Next
    'Halt on error
    Else
        MsgBox "z is infinite"
        End
    End If
End If

'Third column reduction
For i1 = 0 To 3
    If i1 <> 2 Then
        r = Matrix(i1, 2) / Matrix(2, 2)
        For i2 = 0 To 4
            Matrix(i1, i2) = Matrix(i1, i2) - r * Matrix(2, i2)
        Next
    End If
Next

'If w in row4 is zero then error
If Matrix(3, 3) = 0 Then
    MsgBox "W is infinite. Halting"
    End
End If

'Fourth column reduction
For i1 = 0 To 3
    If i1 <> 3 Then
        r = Matrix(i1, 3) / Matrix(3, 3)
        For i2 = 0 To 4
            Matrix(i1, i2) = Matrix(i1, i2) - r * Matrix(3, i2)
        Next
    End If
Next

'Normalize rows
For i1 = 0 To 3
```

```
    r = Matrix(i1, i1)
    For i2 = 0 To 4
        Matrix(i1, i2) = Matrix(i1, i2) / r
    Next
Next

'MsgBox (Matrix(0, 0) & " : " & Matrix(0, 1) & " : " & Matrix(0, 2) & " : " & Matrix(0, 3) & " : " & Matrix(0, 4))
'MsgBox (Matrix(1, 0) & " : " & Matrix(1, 1) & " : " & Matrix(1, 2) & " : " & Matrix(1, 3) & " : " & Matrix(1, 4))
'MsgBox (Matrix(2, 0) & " : " & Matrix(2, 1) & " : " & Matrix(2, 2) & " : " & Matrix(2, 3) & " : " & Matrix(2, 4))
'MsgBox (Matrix(3, 0) & " : " & Matrix(3, 1) & " : " & Matrix(3, 2) & " : " & Matrix(3, 3) & " : " & Matrix(3, 4))


End Sub

Function genI(ByVal Vi As Double, ByVal Delta As Double, ByVal Z As Double, ByVal Gamma As Double, ByVal C As Double) As Double

Dim i3 As Single                                'Riemann counter

Dim A, B As Double    'Transmission and Reflection coefficents
Dim al, be, nu, gg, A1, B1, x, y As Double  'Density of States

Dim Arg1, Arg2, r As Double

genI = 0

'Integrate from 0 to V
If Vi <> 0 Then
    'For i3 = LowerB To UpperB Step RStep
    For i3 = -5 * Kb * T To Vi + 5 * Kb * T Step RStep

        'Current=Current + Stepsize*Function(1+A-B) from BTK theory where E=i3
        x = (i3 ^ 2 + Gamma ^ 2) ^ 2 + Delta ^ 2 * (Gamma ^ 2 - i3 ^ 2)
        y = -2# * Gamma * i3 * Delta ^ 2

        'If x >= 0 Then
            A1 = (((x ^ 2 + y ^ 2) ^ 0.5 + x) / 2#) ^ 0.5
            'B1 = y / (2 * ((x ^ 2 + y ^ 2) ^ 0.5 + x)) ^ 0.5
            B1 = y / (2# * A1)
        'Else
            'B1 = (((x ^ 2 + y ^ 2) ^ 0.5 + Abs(x)) / 2#) ^ 0.5
        '    'B1 = y / (2 * ((x ^ 2 + y ^ 2) ^ 0.5 + x)) ^ 0.5
            'A1 = y / (2# * B1)
        'End If

        al = 0.5 + 0.5 * A1 / (i3 ^ 2 + Gamma ^ 2)
        be = 1 - al
        nu = 0.5 * B1 / (i3 ^ 2 + Gamma ^ 2)

        gg = (al + Z ^ 2 * (al - be)) ^ 2 + (nu * (2 * Z ^ 2 + 1)) ^ 2

        A = ((al ^ 2 + nu ^ 2) * (be ^ 2 + nu ^ 2)) ^ 0.5
        A = A / gg
        B = Z ^ 2 * (((al - be) * Z - 2 * nu) ^ 2 + (2 * nu * Z + (al - be)) ^ 2)
        B = B / gg

        Arg1 = (i3 - Vi) / (Kb * T)
        Arg2 = (i3) / (Kb * T)

        If Arg1 > 100 Then
            r = Exp(-1# * Arg1)
        Else
            r = 1# / (Exp(Arg1) + 1#)
        End If

        If Arg2 > 100 Then
            r = r - Exp(-1# * Arg2)
        Else
            r = r - 1# / (Exp(Arg2) + 1#)
        End If

        genI = genI + RStep * (1 + A - B) * r
    Next
End If

genI = genI * (1# + Z ^ 2) * C / elec


'Check Data
'MsgBox (vi & " : " & genI)

'Output data to file
'Open App.Path & "\IVOut.txt" For Output As #1
```

```
'For i3 = 0 To Points
'    Print #1, v(i3) & " " & genI
'Next
'Close #1

End Function
```

Appendix B

Source Code for the BCS Fits

```
{'Author: Mike Potalivo
'Program Name: LM1para-BCS
'Purpose:  To take different temperatures and deltas, and fit the BCS curve to it.
'It uses the Levenberg-Marquardt method to optimize Delta_0 (or Tc)
'Input: Temperature (K) and delta (mV)
'Outputs:  1 - Input data with new calculated Deltas (mv)
'  2 - Saved Delta_0 from fit                          '


Option Explicit

Const elec As Double = 1.602176462E-19      'Charge of proton
Const Kb As Double = 1.3806503E-23          'Boltzmann Constant
Const Pi As Double = 3.141592654

Private Sub cmdCalc_Click()

Const IterMax As Long = 0          'Maximum iterations allowed
Const Sconverge As Single = 0.001   'Stopping parameter, convergence when abs(SumOld-SumNew)/SumNew <Sconverge
Const SConStop As Integer = 2                'Guarentee convergence. amount of times convergence must be reached

Dim i1, i2 As Long      'For loop counters
Dim i3 As Integer      'Counter
Dim L As Double         'Lambda (LM parameter)
Dim A(0) As Double      'Fitting parameters (Delta0)
Dim x(25) As Double      'X Data
Dim y(25) As Double      'Y Data
Dim yT0(25) As Double     'Theoritically generated y points
Dim yT(25) As Double     'Theoritically generated y points
Dim Sum(1) As Double    'Sum of Squares (old and new)
Dim N As Integer        'Number of data points - 1
Dim M(0, 1) As Double   'Alpha (alpha and Beta parameters matrix parameters)
Dim Data(25) As String      'Lines of Data file

'*************************************************************************
'*****************************     INITIALIZATION     ********************
'*************************************************************************

cmdCalc.Enabled = False

'Initial Guessses
A(0) = 3.5 / 2# * Kb * 1.75 'Delta in terms of Tc=1.75

'Initial Lambda
L = 0.001

'Load in data
N = 0
Open App.Path & "\CuTiSeb\CuTiSe_BCS.txt" For Input As #1
Do While EOF(1) = False
    Input #1, Data(N)
    N = N + 1
Loop
Close #1

i1 = 0
Do
    i2 = InStr(Data(i1), " ")
    i3 = InStr(i2 + 1, Data(i1), " ")
    x(i1) = Val(Left$(Data(i1), i2))
    y(i1) = Val(Mid$(Data(i1), i2, (i3 - i2))) / 1000# * elec

    MsgBox (x(i1) & " : " & y(i1))

    i1 = i1 + 1
Loop While i1 < N

N = i1 - 1
i3 = 0
```

```
MsgBox (N)

'*************************************************************************
'**********************************      PROCEDURE      ******************
'*************************************************************************

'Calculate sum of squares
Sum(0) = 0
For i1 = 0 To N
    yT0(i1) = genI(x(i1), A(0))
    Sum(0) = Sum(0) + (y(i1) - yT(i1)) ^ 2
Next i1

'Loop until convergence or too many iterations
For i2 = 0 To IterMax - 1

    cmdCalc.Caption = "Iteration: " & i2 + 1
    cmdCalc.Refresh

    'Generate Linear Equations for LM
    Call GenerateEqns(M, A, N, L, x, y, yT0)

    'Solve Linear Equations to extract amount to change parameters
    Call Gauss(M)

    'Calc new sum of squares
    Sum(1) = 0
    For i1 = 0 To N
        'yT(i1) = genI(x(i1), A(0) + M(0, 3), A(1) + M(1, 3), A(2) + M(2, 3))
        yT(i1) = genI(x(i1), A(0) + M(0, 1))
        Sum(1) = Sum(1) + (y(i1) - yT(i1)) ^ 2
    Next

    'Compare Sums and make choices
    If Sum(1) >= Sum(0) Then
        'New is worse than old increase Lambda and go again
        L = L * 10#
    Else
        'New is better, save values and decrease Lambda and go again
        L = L / 10#

        'Accept the new coefficent values
        A(0) = A(0) + M(0, 1)

        'Accept the new theoritical y values WRT the new coefficents
        For i1 = 0 To N
            yT0(i1) = yT(i1)
        Next

        lblSum.Caption = "DiffSum: " & Sum(0) - Sum(1)
        lblSum.Refresh

        If (Sum(0) - Sum(1)) / Sum(1) < Sconverge Then
            i3 = i3 + 1
            If i3 = SConStop Then
                MsgBox ("Sum of squares has converged.  Exiting")
                Exit For
            End If
        End If

        Sum(0) = Sum(1)

    End If

    lblL.Caption = "Lambda: " & L
    lblL.Refresh
    lblSum0.Caption = "Sum: " & Sum(0)
    lblSum0.Refresh

    lblDelta.Caption = "Delta0: " & A(0) * 1000# / elec & " meV"
    lblDelta.Refresh
    lblDeltaChange.Caption = "Change in Delta0: " & M(0, 1) * 1000# / elec & " meV"
    lblDeltaChange.Refresh

    Form1.Refresh

    If L > 10000000000# Then
        MsgBox ("There could have been trouble converging")
        Exit For
    End If

Next
```

```
If i2 >= IterMax Then
    MsgBox ("Failure to converge.  Too Many iterations!")
End If

'Output coefficents
'MsgBox ("iterations= " & i2 + 1)
'MsgBox (Sum(0) & " : " & Sum(1))
'MsgBox ("lambda= " & L)
MsgBox ("Delta0= " & A(0) * 1000 / elec & " meV")
'MsgBox ("Z= " & Abs(A(0)))
'MsgBox ("C= " & A(1))
'MsgBox ("T= " & T & " K")

'Output data to file
i1 = 0
Open App.Path & "\CuTiSeb\Fit_BCS.txt" For Output As #1
    Do
        Print #1, x(i1) & " " & 1000 / elec * y(i1) & " " & 1000 / elec * yT0(i1)
        i1 = i1 + 1
    Loop While i1 <= N
Close #1

'Save parameters
Open App.Path & "\CuTiSeb\Report_BCS.txt" For Output As #1
    Print #1, "BCS"
    Print #1, "Delta0: " & A(0) / elec * 1000 & " meV"
Close #1

cmdCalc.Caption = "Calculate"
cmdCalc.Enabled = True

MsgBox ("Finished")
End

End Sub

Sub GenerateEqns(ByRef A() As Double, ByRef C() As Double, ByRef N As Integer, ByRef L As Double, ByRef x() As Double, ByRef_
_y() As Double, ByRef yT() As Double)

Dim i1, i2 As Integer  'Counters

Dim dyda As Double 'Holders of values
Dim h As Double

h = 100#

'Reset M
For i1 = 0 To 0
    For i2 = 0 To 1
        A(i1, i2) = 0
    Next
Next

'Generate Alpha matrix and Beta vector
For i1 = 0 To N

    'dyda = gendIdd(x(i1), C(0), C(1))
    'dydb = gendIdZ(x(i1), C(0), C(1))

    'Numerical derivatives
    'dyda = (genI(x(i1), C(0) + C(0) / h, C(1), C(2)) - genI(x(i1), C(0) - C(0) / h, C(1), C(2))) / (2 * C(0) / h)
    dyda = (genI(x(i1), C(0) + C(0) / h) - genI(x(i1), C(0) - C(0) / h)) / (2 * C(0) / h)

    'dyda = x(i1)
    'dydb = 1

    'Alphas
    A(0, 0) = A(0, 0) + dyda ^ 2

    'Betas
    A(0, 1) = A(0, 1) + (y(i1) - yT(i1)) * dyda

Next i1

'Diagonal Terms
A(0, 0) = A(0, 0) * (1 + L)

End Sub

Sub Gauss(ByRef Matrix() As Double)

Dim Temp(3) As Double
```

```
Dim i1, i2 As Integer
Dim R As Double

'Normalize rows
For i1 = 0 To 0
    R = Matrix(i1, i1)
    For i2 = 0 To 1
        Matrix(i1, i2) = Matrix(i1, i2) / R
    Next
Next

'MsgBox (Matrix(0, 0) & " : " & Matrix(0, 1) & " : " & Matrix(0, 2))
'MsgBox (Matrix(1, 0) & " : " & Matrix(1, 1) & " : " & Matrix(1, 2))

'End

End Sub

Function genI(ByVal T As Double, ByVal DeltaZero As Double) As Double

Dim LS, RS As Double
Dim RStep As Double
Dim x As Double

Dim Convergence As Boolean
Dim Diff As Double
Dim Delta As Double
Dim DeltaSave As Double
Dim Shift As Double
'Dim SmallerDelta As Boolean


'Try a Delta (start at Delta = Delta(0))
Delta = DeltaZero
Diff = 10000000000#
'Shift = -1# * DeltaZero / 10#
'SmallerDelta = True
Convergence = False

Do
    'Solve LS.
    LS = Log(DeltaZero / Delta)

    'Solve RS.
    RStep = (Pi / 2 - 0) / 5000
    RS = 0
    If T <> 0 Then
        For x = 0 + RStep / 2# To Pi / 2 Step RStep
            If Delta / (2 * Kb * T * Cos(x)) < 100 Then

                RS = RS + 2 / Cos(x) * (1 / (Exp(Delta / (Kb * T * Cos(x))) + 1)) * RStep
            Else
                RS = RS + 2 / Cos(x) * Exp(-1# * Delta / (Kb * T * Cos(x))) * RStep
            End If
        Next
    Else
        RS = 0
    End If

    'Search for when LS=RS or closest value
    If Abs(LS - RS) < Diff Then
        Diff = Abs(LS - RS)
        genI = Delta
        DeltaSave = Delta
    Else
        Convergence = True
    End If

    'If Diff = 0 Then  'Or Abs(Shift) < DeltaZero / 10000# Then
    '    Convergence = True
    'End If

    'If LS < RS Then
    '    Shift = -1# * Abs(Shift)
    '    If SmallerDelta = False Then
    '        Shift = Shift / 10#
    '    End If
    '    SmallerDelta = True
    'Else
    '    Shift = Abs(Shift)
    '    If SmallerDelta = True Then
    '        Shift = Shift / 10#
    '    End If
```

```
    '    SmallerDelta = False
    'End If

    'Step through various Deltas
    Delta = Delta - DeltaZero / 500#
    'Delta = Delta + Shift

    'If Delta < 0 Then
    '    Delta = 0
    '    Convergence = True
    '    genI = 0
    'End If

    'MsgBox (Delta & " : " & Diff)

'Loop While Convergence = False
Loop While Delta > 0 And Diff <> 0

End Function
```

Appendix C

Sample of a and c Lattice Parameter Calculations

```
-----------------------------------------------------------
| ***  CuTiSe2 Hot 0.23 Coll3
-----------------------------------------------------------

                              INPUT DATA
                              **********
        EXPERIMENTAL                              EXPERIMENTAL
          2-THETA                                   ERROR

            14.668                                   .250
            29.577                                   .250
            32.679                                   .250
            41.981                                   .250
            45.130                                   .250
            51.512                                   .250
            54.549                                   .250
            60.630                                   .250
            61.501                                   .250
            62.520                                   .250
            68.660                                   .250
            69.250                                   .250
            70.900                                   .250
            78.370                                   .250
            84.520                                   .250
            86.840                                   .250

                  ****************************************

  ---  PARAMETER LIMITS  ---  -------  VOLUME LIMITS  ---------
 |                         | |                                 |
 |    A MAXIMUM = 10.00 A  | |                                 |
 |                         | | VOLUME MINIMUM =     .00 A**3 |
 |    B MAXIMUM = 10.00 A  | |                                 |
 |                         | | VOLUME MAXIMUM = 1000.00 A**3 |
 |    C MAXIMUM = 10.00 A  | |                                 |
 |                         | |                                 |
 ---------------------------- ---------------------------------

    WAVELENGTH = 1.540560

    LOWER FIGURE OF MERIT REQUIRED FOR PRINTED SOLUTION(S) :
M( 16) =   5.0

 ***********************************************************
 **                                                       **
 **  ATTENTION  : VOS DONNEES SONT-ELLES IRREPROCHABLES ?  **
 **  WARNING    : ARE YOUR DATA IRREPROACHABLE ?    **
 **                                                       **
 ***********************************************************

SEARCH OF TETRAGONAL AND/OR HEXAGONAL AND/OR ORTHORHOMBIC
SOLUTION(S)
***********************************************************

  VOLUME DOMAIN BEING SCANNED :
  ============================
 LOWER BOUND =      .00 A**3     HIGHER BOUND =  400.00 A**3

       HEXAGONAL SYSTEM
       ----------------

                H E X A G O N A L   S Y S T E M

DIRECT PARAMETERS : A= 3.54030 C= 6.02513 VOLUME= 65.40
STANDARD DEVIATIONS :   .00253     .00365
```

```
H K L  DOBS    DCAL   DOBS-DCAL QOBS  QCAL 2TH.OBS 2TH.CAL DIF.2TH.
0 0 1 6.03416 6.02513  .00903 .02746 .02755 14.668 14.690 -.022
0 0 2 3.01773 3.01257  .00516 .10981 .11019 29.577 29.629 -.052
1 0 1 2.73801 2.73254  .00547 .13339 .13393 32.679 32.746 -.067
1 0 2 2.15034 2.14884  .00150 .21626 .21657 41.981 42.012 -.031
0 0 3 2.00734 2.00838 -.00104 .24817 .24792 45.130 45.105  .025
1 1 0 1.77263 1.77015  .00249 .31824 .31914 51.512 51.590 -.078
1 0 3 1.68090 1.68002  .00088 .35393 .35430 54.549 54.580 -.031
1 1 2 1.52605 1.52618 -.00013 .42940 .42933 60.630 60.624  .006
0 0 4 1.50651 1.50628  .00023 .44061 .44074 61.501 61.511 -.010
2 0 1 1.48438 1.48566 -.00128 .45385 .45307 62.520 62.460  .060
2 0 2 1.36585 1.36627 -.00043 .53604 .53571 68.660 68.636  .024
1 0 4 1.35564 1.35194  .00370 .54414 .54712 69.250 69.467 -.217
1 1 3 1.32809 1.32796  .00012 .56695 .56706 70.900 70.908 -.008
2 0 3 1.21913 1.21857  .00056 .67282 .67344 78.370 78.413 -.043
1 1 4 1.14540 1.14717 -.00176 .76222 .75988 84.520 84.360  .160
1 0 5 1.12067 1.12151 -.00085 .79625 .79504 86.840 86.758  .082

         * NUMBER OF LINES
              .- INPUT DATA =  16
              .- CALCULATED =  22

         * MEAN ABSOLUTE DISCREPANCIES
                                              <Q> = .7118E-03
                                <DELTA(2-THETA)> = .5714E-01
              MAX. ERROR ACCEPTED (DEG. 2-THETA) = .2650E+00


         * FIGURES OF MERIT
               1.- M( 16) =   25.4              (REF. 4)
               2.- F( 16) =   12.7( .0571,  22)  (REF. 5)

                                        ---------

  ITERATION NUMBER AT EACH DICHOTOMY LEVEL : 1 1 2 2 1 1 1

  VOLUME DOMAIN BEING SCANNED :
  ============================
  LOWER BOUND =  400.00 A**3  HIGHER BOUND =  800.00 A**3

       HEXAGONAL SYSTEM
       ----------------


  ITERATION NUMBER AT EACH DICHOTOMY LEVEL : 0 0 0 0 0 0 0

                                   NO SOLUTION

  VOLUME DOMAIN BEING SCANNED :
  ============================
    LOWER BOUND =  800.00 A**3  HIGHER BOUND = 1000.00 A**3

       HEXAGONAL SYSTEM
       ----------------


  ITERATION NUMBER AT EACH DICHOTOMY LEVEL : 0 0 0 0 0 0 0

                                   NO SOLUTION

  END OF SEARCH FOR TETRAGONAL AND/OR HEXAGONAL
 AND/OR ORTHORHOMBIC SOLUTION(S)
 ************************************************************

---  CALCULATION TIME FOR SEARCH DOWN TO ORTHORHOMBIC SYMMETRY:
    3.070 SEC.

  ---  T O T A L   CALCULATION TIME :     3.0700 SEC.

             DICVOL91 : USEFUL REFERENCES
             --------
  * LOUER, D. & LOUER, M. (1972). J. APPL. CRYST. 5, 271-275.
  * BOULTIF, A. & LOUER, D. (1991). J. APPL. CRYST. 24, 987-993.
```